

Dispersion effects in the miscible displacement of two fluids in a duct of large aspect ratio

By J. ZHANG¹ AND I. A. FRIGAARD^{1,2†}

¹Department of Mathematics, University of British Columbia, 1984 Mathematics Road, Vancouver, BC, V6T 1Z2, Canada

²Department of Mechanical Engineering, University of British Columbia, 2324 Main Mall, Vancouver, BC, V6T 1Z4, Canada

(Received 16 March 2005 and in revised form 1 August 2005)

We study miscible displacements in long ducts in the dispersive limit of small εPe , where $\varepsilon \ll 1$ is the inverse aspect ratio and Pe the Péclet number. We consider the class of generalized Newtonian fluids, with specified closure laws for the fluid properties of the concentration-dependent mixture. Regardless of viscosity ratio and the constitutive laws of the pure fluids, for sufficiently small εPe these displacements are characterized by rapid cross-stream diffusion and slow streamwise dispersion, i.e. the concentration appears to be near-uniform across the duct and spreads slowly as it translates. Using the multiple-scales method we derive the leading-order asymptotic approximation to the average fluid concentration \bar{c}_0 . We show that \bar{c}_0 evolves on the slow timescale $t \sim (\varepsilon Pe)^{-1}$, and satisfies a nonlinear diffusion equation in a frame of reference moving with the mean speed of the flow. In the case that the two fluids have identical rheologies and the concentration represents a passive tracer, the diffusion equation is linear. For Newtonian fluids we recover the classical results of Taylor (1953), Aris (1956), and for power-law fluids those of Vartuli *et al.* (1995). In the case that the fluids differ and/or that mixing is non-passive, \bar{c}_0 satisfies a nonlinear diffusion equation in the moving frame of reference. Given a specific mixing/closure law for the rheological properties, we are able to compute the dispersive diffusivity $D_T(\bar{c}_0)$ and predict spreading along the channel. We show that $D_T(\bar{c}_0)$ can vary significantly with choice of mixing law and discuss why. This also opens the door to possibilities of controlling streamwise spreading by the rheological design of reactive mixtures, i.e. including chemical additives such that the rheology of the mixture behaves very differently to the rheology of either pure fluid. Computed examples illustrate the potential effects that might be achieved.

1. Introduction

The study of miscible displacements in long ducts has received much attention in recent years. Interest comes from Hele-Shaw-type flows, the flow in capillaries and flow in porous media. Displacement processes within these geometries occur in industrial, geophysical and biomedical applications, and for many of these the fluids involved are typically non-Newtonian. The aim of this paper is to study such displacements in the dispersive limit, $\varepsilon Pe \rightarrow 0$ with $Pe \gtrsim 1$, where $\varepsilon \ll 1$ is the inverse aspect ratio. Here the Péclet number Pe is based on the mean fluid velocity and

† Author to whom correspondence should be addressed.

the lengthscale of the duct cross-section, e.g. the radius. Molecular diffusivities are typically in the range, $\hat{D} \lesssim 10^{-9} \text{ m}^2 \text{ s}^{-1}$, and therefore $Pe \gg 1$ is common in miscible fluid–fluid displacements. The dispersive limit corresponds to either a sufficiently long duct and/or to waiting for a sufficiently long time for molecular diffusion to spread fluid concentrations across the duct.

The study of miscible displacements in long ducts has occurred more recently than that of immiscible displacements, which dates back (at least) to the classical studies of Saffman & Taylor (1958); Taylor (1961); Cox (1962). Miscible displacements were first studied in depth within the context of Hele-Shaw and porous-media displacement instabilities, initially motivated by a desire to better understand oil reservoir recovery issues, e.g. Tan & Homsy (1986); Hickernell & Yortsos (1986); Chang & Slattery (1986); Yortsos (1987); Tan & Homsy (1988); Yortsos & Zeybek (1988); Zimmerman & Homsy (1992); Manickam & Homsy (1993); Rogerson & Meiburg (1993 *a, b*). Many of these early works considered instability of displacement fronts, either via classical methods of perturbation about a base state, or with two-dimensional numerical simulations, usually modelling the displacement process by use of a concentration/tracer, i.e. a convection–diffusion equation. The primary focus of these studies is on instability and viscous fingering, and therefore they are generally focused at the short-time behaviour.†

Miscible displacements through capillary ducts have been studied in detail, both experimentally and numerically. For experimental studies, large Pe is usual due to the small molecular diffusivities found with common liquids. For example Petitjeans & Maxworthy (1996) study displacements over a range of Péclet, Atwood (At) and Stokes-buoyancy numbers, using a glycerine–water system which only can give Pe in the range $Pe \gtrsim 400$. For the large- Pe regime, depending on At (or viscosity ratio m), quasi-steady viscous fingers may form and propagate with a sharp displacement front that is retained over $O(1)$ timescales, or longer. A mix of experimental, computational and asymptotic methods have been used to study this regime; the reader is referred to Rakotomalala, Salin & Watzky (1997); Yang & Yortsos (1997), Lajeunesse *et al.* (1997, 1999), Lajeunesse (1999), Scoffoni, Lajeunesse & Homsy (2001), Lajeunesse *et al.* (2001). As $Pe \rightarrow \infty$, those displacements that are stable appear to approach the analogous immiscible fluid results, as has been shown experimentally, as well as in a formal asymptotic sense and computationally; see e.g. Petitjeans & Maxworthy (1996), Chen & Meiburg (1996), Rakotomalala *et al.* (1997), Yang & Yortsos (1997). For example, Yang & Yortsos (1997) consider asymptotic solutions to the problem of miscible displacement in long ducts (represented in our notation by $\varepsilon \ll 1$). They consider the limit that $\varepsilon \rightarrow 0$ with εPe fixed. Their leading-order transverse flow equilibrium (TFE) model combines a lubrication approximation for the velocity, with a convection–diffusion equation for the fluid concentration, containing only cross-stream diffusion. The TFE model is attractive as the simplest two-dimensional model that can adequately reproduce effects observed in more complete two-dimensional computational models of miscible displacements. Yang & Yortsos (1997) present computed solutions of the TFE model, for a variety of viscosity ratios $0.01 \leq m \leq 100$, and over the range $\varepsilon Pe \in [0.025, \infty)$. Analytically, they study the immiscible limit of their TFE model, $\varepsilon Pe \rightarrow \infty$, for which they derive a lubrication model that is formally

† The more rudimentary form of this type of work dates back to Muskat (1937) and it is worth mentioning that numerous applications of such analyses can be found in the technical literature pertaining to oil production.

equivalent to that for immiscible fluids with zero surface tension (see also Lajeunesse *et al.* (1999), Lajeunesse (1999) for a similar approach).

Our paper considers instead the dispersive limit of miscible displacements. A first problem is to clearly define what is the correct dispersive limit of these flows. In the results of Chen & Meiburg (1996), at low Pe , the displacement front between fluids is observed to become increasingly diffuse at the tip and the concentration diffuses relatively quickly across the duct. After times, $t \sim Pe$, Chen & Meiburg (1996) show that the axial gradient of the mean concentration approaches a Gaussian shape. This resembles the results of the classical studies of Taylor (1953) and Aris (1956) for passive tracers, strongly hinting that the displacement process becomes dispersive at long enough times. Yang & Yortsos (1997) show that when $\varepsilon Pe \lesssim 1$, even for extreme viscosity ratios, the concentration contours become nearly uniform across the duct. However, Yang & Yortsos' dual limit: $\varepsilon \rightarrow 0$ at fixed εPe , followed by $\varepsilon Pe \rightarrow 0$, is not the limit we consider. Even for large Pe (assuming stability), we expect to enter the dispersive regime if we wait long enough for cross-stream diffusion to mix across the duct and hence affect axial propagation via dispersion. In a long duct the aspect ratio is indicative of the (dimensionless) timescale required to travel the length of the duct. The limit $\varepsilon Pe \rightarrow 0$, at fixed Pe , therefore allows time for dispersive effects to dominate, i.e. $\varepsilon Pe \ll 1$ implies that on the convective timescale, relevant to passage down the duct, the distance diffused across the stream is much larger than the duct radius. Viewed another way, εPe is the ratio of timescales for diffusion across the channel to advection down the channel. Typically we shall also consider $Pe \gtrsim 1$, since anyway this is the range of interest for most liquid–liquid displacements.

Although we define $\varepsilon Pe \rightarrow 0$, at fixed $Pe \gtrsim 1$, as the dispersive limit, dispersive effects are almost certainly dominant for other parameter regimes outside this limit, due to instability-driven mixing. For example, at high flow rates and for certain conditions on the viscosity ratio m , different displacement front instabilities occur, which have been classified experimentally by Lajeunesse *et al.* (1997, 1999), Lajeunesse (1999), Lajeunesse *et al.* (2001). In practice, not only frontal instabilities are likely to occur. As reported by Chen & Meiburg (1996), high- Pe viscous fingers persist over a timescale of order Pe before diffusive effects smear the interface and ‘choke’ the flow of pure fluids in the layers. Before this, over intermediate timescales the sides of quasi-steady evolving fingers become approximately parallel to the duct walls and a (near-) parallel multi-layer shear flow is found. Such flows are often vulnerable to interfacial instabilities; see e.g. Joseph & Renardy (1993) for a review. Recent work by Ern, Charru & Luchini (2003) has considered miscible fluids in which the viscosity varies rapidly between two constant values, (essentially the large- Pe regime). They show that ‘interfacial’ instabilities do arise as the immiscible limit is approached. We may expect that mixing timescales are $O(1)$ once interfacial instabilities are initiated. There are also other complications in understanding when results that show stably evolving fingers over long timescales are realistic. For example, what are the effects of neglecting Korteweg stresses, and of potential anisotropy in the porous-media case, how well does the concentration–convection–diffusion formalism model these flows, etc. Such questions have been partly addressed by Zimmerman & Homsy (1992), Chen & Meiburg (1996, 2002).

In this paper we use the multiple-scales method to derive an asymptotic approximation to the leading-order-concentration field, in the limit $\varepsilon Pe \rightarrow 0$, at fixed $Pe \gtrsim 1$. The asymptotic analysis of this problem appears new, although Yang & Yortsos (1997) do briefly consider the case of large diffusion, i.e. taking $\varepsilon Pe \rightarrow 0$ in their TFE model, ($\varepsilon \rightarrow 0$). Their perturbation expansion leading to the TFE model

breaks down and it becomes necessary to (artificially) reintroduce axial diffusion. They then proceed to show that the concentration diffuses axially in a frame of reference moving with the mean speed, as with classical Taylor dispersion. However, Yang & Yortsos' model does not recover the Taylor dispersion coefficient for the diffusion of the mean concentration in the case of a passive tracer, which it obviously should do.

The method that we propose has general application, requiring only the specification of smooth closure laws for the fluid rheological properties as a function of the concentration. In the case that the two fluids are identical, we recover the usual results for Taylor dispersion. When the fluid properties are not the same, we shall find instead a nonlinear diffusion equation modelling the axial distribution of the mean fluid concentration. Our study considers not only Newtonian fluids but also generalized Newtonian and yield-stress fluids, since these may be treated identically.

The literature for non-Newtonian displacements is less developed than that for Newtonian displacements. We later focus specifically on duct displacements, not on porous-media displacements. This distinction needs to be made more strictly for non-Newtonian fluids than for Newtonian fluids. Although nonlinear flow curves are found for the flow of non-Newtonian fluids through porous media, see e.g. Barenblatt, Entov & Ryzhik (1990), the analogy between porous-media flow and a related Hele-Shaw (or Poiseuille) flow is harder to establish. What this means practically is that the flow curve parameters that characterize the nonlinear Darcy relation are unlikely to be readily identified with rheological parameters governing pressure-driven flow down a duct, even though, for example, a shear-thinning fluid is likely to produce shear-thinning behaviour in both cases. One approach to this averaging/homogenization procedure is explored by Liu & Masliyah (1999). A detailed consideration of the inherent problems can be found in Tardy & Pearson (2002). Studies of displacement instabilities in porous media have been made for yield-stress fluids by Pascal (1984*a, b*, 1986), and for shear-thinning fluids (power-law and Carreau models) by Azaiez & Singh (2002).

There also have been numerous studies of viscous fingering with non-Newtonian fluids in the classical Hele-Shaw geometries, experimental as well as analytical. An incomplete list (with apologies), includes Nittmann, Daccord & Stanley (1985), Daccord, Nittman & Stanley (1986), Wilson (1990), Sade, Chan & Hughes (1994), Kondic, Shelley & Palfy-Muhoray (1996), Alexandrou & Entov (1997), Kawaguchi, Makino & Kato (1997), Kondic, Palfy-Muhoray & Shelly (1998), Coussot (1999), Lindner (2000), Lindner, Coussot & Bonn (2000). Considering generalized Newtonian fluids and non-Hele-Shaw displacements, in tubes and between parallel plates, the high- Pe limit has been considered in the lubrication limit by Bakhtiyarov & Siginer (1996) and by Allouche, Frigaard & Sona (2000). The propagation of fingers in fully two-dimensional displacement flows of yield-stress fluids is considered both computationally and analytically in Allouche *et al.* (2000), Frigaard, Scherzer & Sona (2001) and Dimakopoulos & Tsamopoulos (2003). Related experimental studies are those of Gabard (2001), Gabard & Hulin (2003). These displacement studies are over short timescales, with no account taken of molecular diffusion in the modelling studies and no significant diffusive effects observed in the experimental work.

A first motivation for this work comes from an ongoing study into the displacement flows that occur in the primary cementing of an oil well, which are characterized by displacements of shear-thinning yield-stress fluids in a long eccentric annulus (e.g. mean gap width $\sim 10^{-2}$ m, typical length 10^2 – 10^3 m). Apart from the occurrence of static (unyielded) residual layers (see Allouche *et al.* 2000; Frigaard *et al.* 2001; Frigaard, Leimgruber & Scherzer 2003), there appears to be little contamination of

the setting cement in successful displacements, which suggests homogeneity of any mixture across the annular gap. This occurs in spite of not being strictly in the dispersive regime as outlined above. This ongoing work is described in Bittleston, Ferguson & Frigaard (2002), Pelipenko & Frigaard (2004*a, b, c*), and is based on a Hele-Shaw approach. An initial motivation for this study was to examine more closely the validity of our modelling strategy. A second motivation is to be able to study the effects on dispersion of, for example, non-monotonic variations in the rheological properties, as might be chemically engineered. We deal with this at the end of the paper.

A final motivation for the work is that this is a limit where an analytic or semi-analytic method should be more effective than a numerical method. Much of the complexity of the high- Pe flows has gone, since the flows mix in the cross-stream direction and become effectively one-dimensional over times $\sim (\varepsilon Pe)^{-1}$. Given specified mixture properties, the challenge is therefore to derive the correct leading-order model. The alternative of solving any two-dimensional problem accurately over such long timescales is problematic. The growth of significant numerical diffusion over the timescale $(\varepsilon Pe)^{-1}$, as $(\varepsilon Pe) \rightarrow 0$, appears to be practically unavoidable. This makes it extremely difficult to delineate the physical processes of diffusion and dispersion from analogous numerical effects in any computed results.

A brief outline of paper is as follows. In §2 we introduce the basic concentration equation model for miscible displacements, and discuss both rheological and mixture closure laws. Section 3 shows computed example results from Yang & Yortsos' TFE model, which help motivate the statement that for small enough εPe , cross-stream diffusion is rapid and axial dispersion dominates the streamwise spreading, regardless of rheological model. Our asymptotic approximation is derived in §4. Section 5 presents results of computing the Taylor dispersion coefficients for the case of passive tracer displacements, for which axial dispersion is modelled by a linear diffusion process. When mixing is non-passive the diffusion process becomes nonlinear, and this is modelled in §6. We first demonstrate the validity of the asymptotic method by comparison with two-dimensional results using the TFE model. Secondly we show how the mixing law can affect axial spreading of the mixture, and indicate how this might be used to minimize spreading. The paper concludes with a short summary.

2. Miscible displacements

Consider miscible displacement of two iso-density non-Newtonian fluids along a plane channel, $\hat{x} \in [-\hat{R}, \hat{R}]$, aligned with the \hat{z} -axis. We suppose a nominal lengthscale \hat{L} in the \hat{z} -direction and assume that the aspect ratio $\hat{L}/\hat{R} \gg 1$. The fluids are incompressible and are pumped at a mean velocity \hat{W}_0 in the \hat{z} -direction, with fluid 2 displacing fluid 1 (the *in situ* fluid). The concentration of fluid 2 will be denoted by c . We adopt a classical lubrication/thin-film scaling for the equations of motion and concentration. After scaling, the dimensionless equations of motion for the velocity, $\mathbf{u} = (u, w)$, and pressure p , are

$$\varepsilon^3 Re \left(\frac{\partial u}{\partial t} + u \frac{\partial u}{\partial x} + w \frac{\partial u}{\partial z} \right) = -\frac{\partial p}{\partial x} + \varepsilon \frac{\partial}{\partial x} \tau_{xx} + \varepsilon^2 \frac{\partial}{\partial z} \tau_{xz}, \quad (2.1)$$

$$\varepsilon Re \left(\frac{\partial w}{\partial t} + u \frac{\partial w}{\partial x} + w \frac{\partial w}{\partial z} \right) = -\frac{\partial p}{\partial z} + \frac{\partial}{\partial x} \tau_{zx} + \varepsilon \frac{\partial}{\partial z} \tau_{zz}, \quad (2.2)$$

$$u_x + w_z = 0, \quad (2.3)$$

where τ_{ij} denotes the scaled deviatoric stress tensor. The dimensionless advection–diffusion equation for the concentration is

$$\varepsilon Pe \left(\frac{\partial c}{\partial t} + u \frac{\partial c}{\partial x} + w \frac{\partial c}{\partial z} \right) = \frac{\partial^2 c}{\partial x^2} + \varepsilon^2 \frac{\partial^2 c}{\partial z^2}. \quad (2.4)$$

The dimensionless numbers above are Re , ε and Pe . Re is the Reynolds number $Re = \hat{R} \hat{W}_0 / \hat{\nu}_2$, where $\hat{\nu}_2$ denotes the kinematic viscosity of pure fluid 2. The inverse aspect ratio is $\varepsilon = \hat{R} / \hat{L} \ll 1$, and $Pe = \hat{R} \hat{W}_0 / \hat{D}$ is the Péclet number, which describes the ratio of timescales for convection and diffusion of mass; \hat{D} is the molecular diffusivity. Later we shall write

$$Re = \frac{Pe}{Sc}, \quad Sc = \frac{\hat{\nu}_2}{\hat{D}}.$$

The Schmidt number, Sc represents the ratio of timescales for mass (molecular) diffusion and momentum diffusion. This enables us to work asymptotically with (εPe). We assume $Sc \geq 1$, which is true for most liquids.

An analogous model may be derived for displacements along a pipe of radius \hat{R} . We avoid repetition and simply state the relevant results, wherever the details are trivial. Throughout the paper we work primarily in dimensionless variables. Dimensional quantities are denoted with a ‘hat’ symbol, e.g. \hat{W}_0 is the dimensional mean velocity.

2.1. Rheological models

We suppose that both fluids and their mixture fall into the class of generalized Newtonian fluids. For such fluids, the rate of strain $\dot{\gamma}_{ij}$ and the deviatoric stress τ_{ij} are related through a constitutive equation of form

$$\tau_{ij} = \eta(\dot{\gamma}) \dot{\gamma}_{ij} \quad \text{with } \dot{\gamma} = \sqrt{\frac{\dot{\gamma}_{ij} \dot{\gamma}_{ij}}{2}}, \quad (2.5)$$

where $\eta = \eta(\dot{\gamma})$ is termed the effective viscosity. After scaling, we find that

$$\dot{\gamma}_{xx} = 2\varepsilon \frac{\partial u}{\partial x} = -2\varepsilon \frac{\partial w}{\partial z} = -\dot{\gamma}_{zz}, \quad \dot{\gamma}_{xz} = \dot{\gamma}_{zx} = \frac{\partial w}{\partial x} + \varepsilon^2 \frac{\partial u}{\partial z}. \quad (2.6)$$

Thus, $\dot{\gamma} \sim |\partial w / \partial x| + O(\varepsilon^2)$, and only the shear stress terms appear at $O(1)$ in the scaled z -momentum equation.

Our analysis is applicable to a wide range of rheological models of form (2.5). For $\dot{\gamma} > 0$, τ should be a strictly increasing function of $\dot{\gamma}$ (and vice versa). If the monotonicity extends to $\dot{\gamma} = 0$ and if $\tau(\dot{\gamma} \rightarrow 0^+) = 0$, then the models are nonlinearly viscous. If instead, $\tau(\dot{\gamma} \rightarrow 0^+) = B > 0$, then the models are visco-plastic, with yield stress B . Here τ denotes the second invariant of the deviatoric stress: $\tau = \sqrt{(\tau_{ij} \tau_{ij})/2}$. Although the analysis is general, we focus on the following three popular models.

(a) Power-law fluid:

$$\eta(\dot{\gamma}) = \dot{\gamma}^{n-1}.$$

Here the kinematic viscosity scale used is $\hat{\nu} = (\hat{K} \hat{W}_0^{n-1}) / (\hat{\rho} \hat{R}^{n-1})$, where \hat{K} is termed the consistency of the fluid and n the power-law index. The dimensionless model is parameterized only by n . For $n < 1$, the fluid is termed shear-thinning or pseudo-plastic; for $n > 1$ the fluid is termed shear-thickening.

(b) Carreau:

$$\eta(\dot{\gamma}) = 1 + (\alpha - 1)(1 + (\beta \dot{\gamma})^2)^{(n-1)/2}.$$

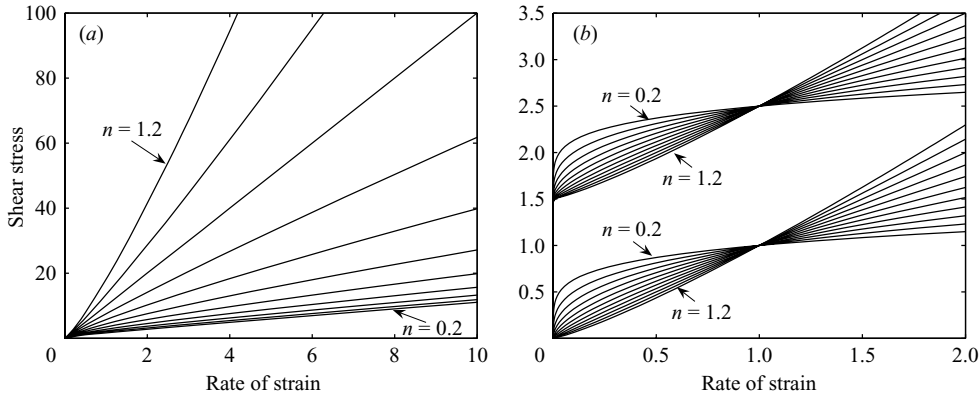


FIGURE 1. Examples of the constitutive models for different values of shear-thinning index $n=0.2, 0.3, 0.4, \dots, 1.2$. (a) Carreau fluid, $\alpha = 10, \beta = 25$; (b) power-law and Herschel–Bulkley models ($B = 1.5$) (lower and upper sets of curves, respectively).

Here the kinematic viscosity scale used is $\hat{v} = \hat{\eta}_\infty / \hat{\rho}$, where $\hat{\eta}_\infty$ is the high-shear viscosity. The two dimensionless parameters α and β are defined by

$$\alpha = \frac{\hat{\eta}_0}{\hat{\eta}_\infty} > 1, \quad \beta = \frac{\hat{\lambda} \hat{W}_0}{\hat{R}},$$

where $\hat{\eta}_0$ is the low-shear viscosity and where $\hat{\lambda}^{-1}$ is a characteristic scale for the range of $\dot{\gamma}$ over which the viscosity drops from $\hat{\eta}_0$ to $\hat{\eta}_\infty$. Thus, α is a viscosity ratio and n is a power-law index, as before. Loosely, the size of β determines whether the transition from high to low viscosity is sharp or not.

(c) Herschel–Bulkley:

$$\begin{aligned} \tau_{ij} &= \left(\dot{\gamma}^{n-1} + \frac{B}{\dot{\gamma}} \right) \dot{\gamma}_{ij} && \text{iff } \tau > B, \\ \dot{\gamma} &= 0 && \text{iff } \tau \leq B. \end{aligned}$$

This is an extension of the power-law model to a fluid with a yield stress, $\hat{\tau}_Y$. The kinematic viscosity scale used is again $\hat{v} = (\hat{K} \hat{W}_0^{n-1}) / (\hat{\rho} \hat{R}^{n-1})$. The additional dimensionless parameter is $B = (\hat{\tau}_Y \hat{R}^n) / (\hat{K} \hat{W}_0^n)$, termed the Bingham number, which denotes the ratio of yield stress to viscous stress. The effective viscosity is defined from $\tau = \eta(\dot{\gamma})\dot{\gamma}$.

Examples of these constitutive relations are shown in figure 1. For all models an appropriate choice of parameters returns the Newtonian model, $\eta = 1$. For the Herschel–Bulkley model, if we set $n = 1$ we recover the popular Bingham model. Note that for the Herschel–Bulkley model, if $B > 0$, then $\eta \rightarrow \infty$ as $\dot{\gamma} \rightarrow 0$.

2.2. Mixing laws

Consider an infinite channel. The situation assumed is that as $z \rightarrow -\infty$ we have $c = 1$, i.e. pure fluid 2 with known rheological law $\eta = \eta_2(\dot{\gamma})$, and as $z \rightarrow \infty$ we have $c = 0$, i.e. pure fluid 1 with known rheological law $\eta = \eta_1(\dot{\gamma})$. In some intermediate zone we have a mixture $c \in (0, 1)$ and must specify the rheology of the mixture.

Since we have used the kinematic viscosity of fluid 2 to provide the viscosity scale, we may write

$$\eta_2(\dot{\gamma}) = \eta(\dot{\gamma}; \mathbf{q}_2),$$

where $\eta(\dot{\gamma}; \mathbf{q}_2)$ is any of the effective viscosity functions in §2.1 and \mathbf{q}_2 denotes a vector of dimensionless rheological parameters (e.g. $\mathbf{q}_2 = (n_2, \alpha_2, \beta_2)$), if fluid 2 were a Carreau fluid). For fluid 1, we will have a different kinematic viscosity scale and therefore

$$\eta_1(\dot{\gamma}) = m\eta(\dot{\gamma}; \mathbf{q}_1),$$

where $\eta(\dot{\gamma}; \mathbf{q}_1)$ is any of the effective viscosity functions in §2.1 and \mathbf{q}_1 is the corresponding vector of dimensionless rheological parameters. The parameter m is the ratio of (kinematic) viscosities between the two pure fluids, e.g. if fluid 1 is a Carreau fluid and fluid 2 is an Herschel–Bulkley fluid, then

$$m = \frac{\hat{v}_1}{\hat{v}_2} = \frac{\hat{\eta}_{1,\infty} \hat{K}^{n-1}}{\hat{K}_2 \hat{W}_0^{n-1}}.$$

Thus, in general we shall assume a closure of form

$$\eta = \eta(\dot{\gamma}; c, \eta_1, \eta_2, m). \quad (2.7)$$

To specify $\eta(\dot{\gamma}; c, \eta_1, \eta_2, m)$ empirically for a pair of liquids requires extensive experimental measurement, which is not the purpose of this paper. The mixture viscosity depends on the characteristics of the mixing process at a molecular level, which may include various reactions between the liquid components. In particular, if one pair of liquid components has an identical rheology to another pair of liquid components (with different chemical composition), it is unlikely that the mixture of the first pair will have an identical rheology to that of the second pair. It is therefore impossible to state a generally applicable physical law. What follows analytically is valid for mixture viscosities that are continuous interpolants between the effective viscosities of the pure fluids, say C^1 with respect to the concentration.

For purposes of computation and illustration, it is however necessary to specify a mixing closure law. What is required computationally is to be able to determine $\dot{\gamma}$ for any given mixture of two specified fluids, at a given stress τ , i.e. $\dot{\gamma}(\tau; c, \eta_1, \eta_2, m)$. Here we will consider two different mixing laws, that we define implicitly as follows:

$$\dot{\gamma}(\tau; c, \eta_1, \eta_2, m) = [(1-c)\dot{\gamma}_1(\tau)^{0.25} + c\dot{\gamma}_2(\tau)^{0.25}]^4, \quad (2.8)$$

$$\dot{\gamma}(\tau; c, \eta_1, \eta_2, m) = (1-c)\dot{\gamma}_1(\tau) + c\dot{\gamma}_2(\tau), \quad (2.9)$$

where the functions $\dot{\gamma}_k(\tau)$, $k=1, 2$ are defined implicitly by

$$\tau = \eta_1(\dot{\gamma}_1; \mathbf{q}_1)\dot{\gamma}_1, \quad (2.10)$$

$$\tau = \eta_2(\dot{\gamma}_2; \mathbf{q}_2)\dot{\gamma}_2. \quad (2.11)$$

Suppose for example that both fluids are Newtonian, with scaled constant viscosities μ_1 and μ_2 (in fact equal to unity, due to our scaling). Then for (2.8) we have

$$\dot{\gamma} = \left[(1-c) \left(\frac{\tau}{m\mu_1} \right)^{0.25} + c \left(\frac{\tau}{\mu_2} \right)^{0.25} \right]^4 \Rightarrow \eta = \frac{\tau}{\dot{\gamma}} = [(1-c)(m\mu_1)^{-0.25} + c\mu_2^{-0.25}]^{-4},$$

and for (2.9) we have

$$\dot{\gamma} = (1-c)\frac{\tau}{m\mu_1} + c\frac{\tau}{\mu_2} \Rightarrow \eta = \frac{\tau}{\dot{\gamma}} = \left[(1-c)\frac{1}{m\mu_1} + c\frac{1}{\mu_2} \right]^{-1}.$$

Therefore, (2.8) can be interpreted as a non-Newtonian extension of a ‘quarter-power’ mixing rule. For two Newtonian fluids, (2.8) is identical to that used by Yang &

Yortsos (1997). The second closure, (2.9), is clearly a non-Newtonian extension of linear interpolation of the fluidity.

3. The TFE model

The transverse flow equilibrium (TFE) model is obtained by taking the formal limit $\epsilon \rightarrow 0$ for ϵPe and Re fixed; see Yang & Yortsos (1997). Aside from inertial instabilities, this model can reproduce the qualitative features of more complex two-dimensional numerical simulations, and in particular those observed at small and large ϵPe . We shall use computed results from this model to motivate the asymptotic approach that we take below in §4. The model consists of the following leading-order system:

$$0 = -\frac{\partial p}{\partial x}, \quad (3.1)$$

$$0 = -\frac{\partial p}{\partial z} + \frac{\partial}{\partial x} \left(\eta \frac{\partial w}{\partial x} \right), \quad (3.2)$$

$$\frac{\partial u}{\partial x} + \frac{\partial w}{\partial z} = 0, \quad (3.3)$$

$$\epsilon Pe \left(\frac{\partial c}{\partial t} + u \frac{\partial c}{\partial x} + w \frac{\partial c}{\partial z} \right) = \frac{\partial^2 c}{\partial x^2}, \quad (3.4)$$

with boundary conditions

$$0 = \frac{\partial c}{\partial x}(0, z, t) = \frac{\partial c}{\partial x}(1, z, t), \quad (3.5)$$

$$0 = \frac{\partial w}{\partial x}(0, z, t) = w(1, z, t), \quad (3.6)$$

$$0 = u(0, z, t) = u(1, z, t). \quad (3.7)$$

Note that this model retains the leading-order coupling between velocity and concentration. The single parameter $(\epsilon Pe)^{-1}$ can be interpreted as a transverse diffusivity (if the reader wishes to compare results with Yang & Yortsos (1997), their transverse diffusivity N_{TD} is defined by $N_{TD}^{-1} = 4\epsilon Pe$). Our main aim in considering the TFE model is to justify the assertion that, regardless of rheological models and viscosity ratios, for sufficiently small ϵPe and over a timescale $t \sim (\epsilon Pe)^{-1}$, the concentration field becomes quasi-uniform across the channel.

3.1. Computational details

We solve the system (3.1)–(3.7) using a high-resolution non-oscillatory central scheme with non-staggered grids for multidimensional hyperbolic conservation laws, as presented in Jiang *et al.* (1998). This scheme is based on the multidimensional non-oscillatory central scheme introduced in Jiang & Tadmor (1998). Our aim is to show that regardless of rheological model and viscosity ratio, for sufficiently small ϵPe we enter a dispersive regime. The TFE model is particularly suitable for this as there is no axial diffusion, so that spreading can only be by dispersion. A high-order method is required to minimize the effects of numerical diffusion. As a numerical experiment, we start at $t=0$ with the channel full of fluid 1. Fluid 2 enters at $z=0$, starting at $t=0$. We show results a short time later, at $t=0.3$.

For all results shown in figures 2–4, concentration contours of the fluid mixture are plotted at values, $c=0.1, 0.2, \dots, 0.9$. A mesh spacing $\Delta x = 1/100$, $\Delta z = 1/100$

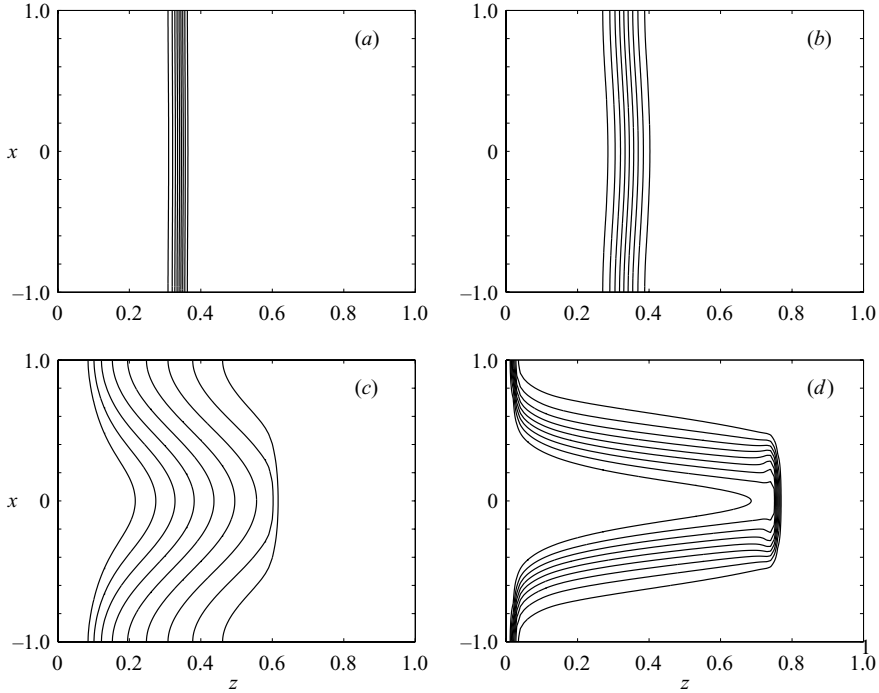


FIGURE 2. Concentration $c(x, z, 0.3)$ for two Newtonian fluids, $m = 100$. (a) $\varepsilon Pe = 0.01$; (b) $\varepsilon Pe = 0.1$; (c) $\varepsilon Pe = 1$; (d) $\varepsilon Pe = 10$.

was used and the timestep was selected to preserve stability of the scheme, typically $\Delta t \sim 10^{-3}$. The main computational work is in solving (3.4). For a given concentration field, at each timestep, (3.2) is integrated numerically at fixed z , to give the shear stress at each position x , for a given constant pressure gradient p_z . For the specified rheological mixture law, τ is inverted to give the rate of strain $\dot{\gamma} = |\partial w / \partial x|$. The velocity w is then found by integrating $\dot{\gamma}$, using the no-slip condition at the wall. This procedure is iterated to find p_z , such that $w(x, z, t)$ has unit average across the channel, at each fixed z . Once $w(x, z, t)$ is found for all (x, z) , the transverse velocity $u(x, z, t)$ is computed from (3.3). For the mixture rheology, we use the quarter-power law (2.8), as in Yang & Yortsos (1997).

3.2. Computational results

Displacements of Newtonian mixtures with viscosity ratio $m = 100$ are shown in figure 2. These results are analogous to results presented in Yang & Yortsos (1997). Displacements at large m are most susceptible to viscous fingering, as we see at large εPe . For even larger values of εPe the displacement profiles approach those of the corresponding immiscible fluid displacement. Also observe that as εPe decreases, concentration gradients across the channel are reduced and the dispersion-dominated regime emerges.

To illustrate the generality of these results, we have computed displacements for pairs of power-law and Herschel–Bulkley fluids. We plot only the results for small εPe , i.e. $\varepsilon Pe = 0.1, 0.01$. A sample of the results is shown in figures 3 and 4. At larger εPe , a variety of complex fingering patterns are found, strongly dependent on the rheologies and viscosity ratio. In all cases that we have computed we see that

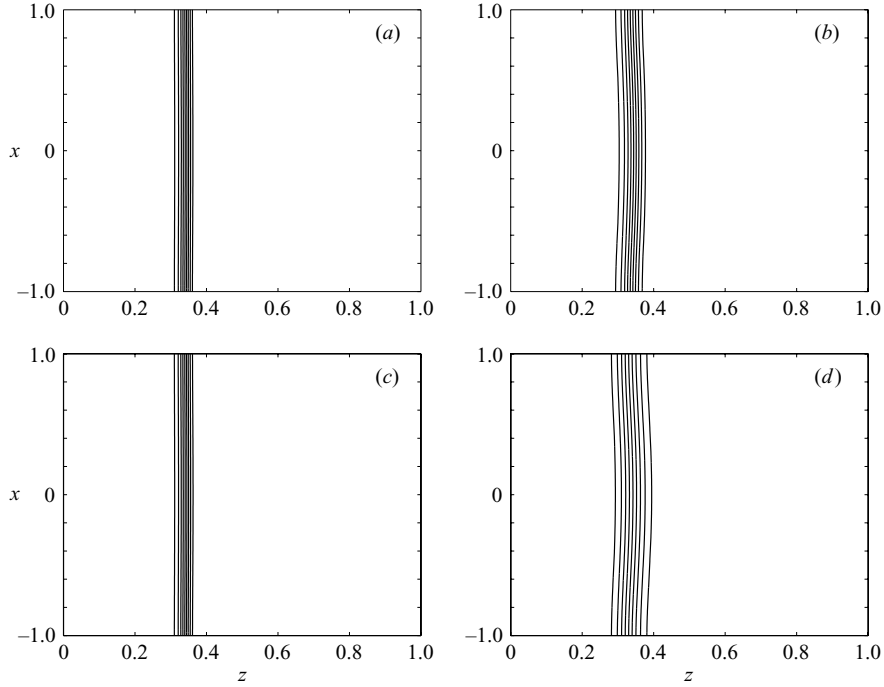


FIGURE 3. Concentration $c(x, z, 0.3)$: two power-law fluids. (a, b) $n_1=0.4$, $n_2=0.8$, $m=0.01$, (a) $\varepsilon Pe=0.01$, (b) $\varepsilon Pe=0.1$; (c, d) $n_1=0.8$, $n_2=0.4$, $m=100$, (c) $\varepsilon Pe=0.01$, (d) $\varepsilon Pe=0.1$.

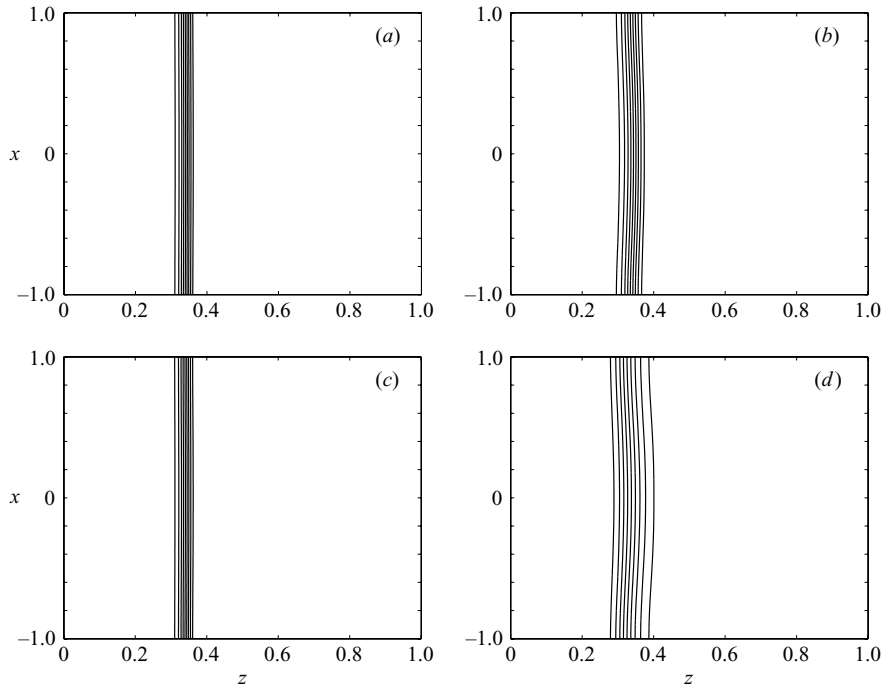


FIGURE 4. Concentration $c(x, z, 0.3)$ for two Herschel-Bulkley fluids. (a, b) $n_1=0.5$, $n_2=1$, $B_1=1$, $B_2=5$, $m=0.01$, (a) $\varepsilon Pe=0.01$, (b) $\varepsilon Pe=0.1$; (c, d) $n_1=1$, $n_2=0.5$, $B_1=5$, $B_2=1$, $m=100$, (c) $\varepsilon Pe=0.01$, (d) $\varepsilon Pe=0.1$.

transverse mixing dominates at small enough εPe , regardless of the fluid rheologies and viscosity ratios.

4. Multiple-scales approximation

In §3, we have seen that for small enough εPe , the concentration gradients are predominantly in the z -direction, i.e. rapid diffusion in the x -direction smooths out transverse concentration gradients. When considered in a moving frame of reference, the mean concentration appears to diffuse slowly along the channel. The observations of §3 are reminiscent of classical Taylor dispersion; see Taylor (1953); Aris (1956). In this section we analyse (2.1)–(2.4), using the method of multiple scales, and derive an asymptotic approximation to the leading-order concentration. The method is suggested by Fowler (1998) as an alternative means of deriving the classical Taylor–Aris dispersion results, but can be generalized, as we shall see below. Our analysis will confirm the diffusive nature of spreading of the leading-order concentration, in a frame of reference convected with the mean flow. We also derive the general expression for the nonlinear dispersive diffusivity, for arbitrary generalized Newtonian fluids and any given mixing law.

4.1. Asymptotic expansion

We shift to a frame of reference $\xi = z - t$, moving with the mean velocity of the flow and define $\delta = \varepsilon Pe$. Next we introduce a slow time $T = \delta t$, and assume that the variables in (2.1)–(2.4) respond independently with respect to t and T . The system (2.1)–(2.4) becomes

$$\frac{\delta^3}{ScPe^2} \left(\frac{\partial u}{\partial t} + \delta \frac{\partial u}{\partial T} + u \frac{\partial u}{\partial x} + \tilde{w} \frac{\partial u}{\partial \xi} \right) = -\frac{\partial p}{\partial x} + O([\delta/Pe]^2), \quad (4.1)$$

$$\frac{\delta}{Sc} \left(\frac{\partial \tilde{w}}{\partial t} + \delta \frac{\partial \tilde{w}}{\partial T} + u \frac{\partial \tilde{w}}{\partial x} + \tilde{w} \frac{\partial \tilde{w}}{\partial \xi} \right) = -\frac{\partial p}{\partial z} + \frac{\partial}{\partial x} \left(\eta \frac{\partial \tilde{w}}{\partial x} \right) + O([\delta/Pe]^2), \quad (4.2)$$

$$\frac{\partial u}{\partial x} + \frac{\partial \tilde{w}}{\partial \xi} = 0, \quad (4.3)$$

$$\delta \left(\frac{\partial c}{\partial t} + \delta \frac{\partial c}{\partial T} + u \frac{\partial c}{\partial x} + \tilde{w} \frac{\partial c}{\partial \xi} \right) = \frac{\partial^2 c}{\partial x^2} + \frac{\delta^2}{Pe^2} \frac{\partial^2 c}{\partial \xi^2}, \quad (4.4)$$

where $\tilde{w} = w - 1$. Note that $\partial w/\partial x = \partial \tilde{w}/\partial x$, $\partial w/\partial z = \partial \tilde{w}/\partial \xi$, etc. The leading-order rate of strain is $\dot{\gamma} \sim |\partial \tilde{w}/\partial x| + O(\varepsilon^2)$, and hence $\eta \sim \eta(|\partial \tilde{w}/\partial x|) + O(\varepsilon^2) = \eta(|\partial \tilde{w}/\partial x|) + O([\delta/Pe]^2)$.

The following boundary conditions in x are satisfied:

$$\frac{\partial c}{\partial x} = 0 \quad \text{at} \quad x = 0, 1, \quad (4.5)$$

$$u = 0 \quad \text{at} \quad x = 0, 1, \quad (4.6)$$

$$\frac{\partial \tilde{w}}{\partial x} = 0 \quad \text{at} \quad x = 0, \quad (4.7)$$

$$\tilde{w} = -1 \quad \text{at} \quad x = 1. \quad (4.8)$$

In addition, since we have subtracted the mean flow,

$$\int_0^1 \tilde{w} \, dx = 0. \quad (4.9)$$

We now assume $\delta \ll 1$, with $Pe \gtrsim 1$. We seek formal asymptotic expansions of c , u , \tilde{w} and p , in powers of δ :

$$\begin{aligned} c(T, t, x, \xi) &= c_0(T, t, x, \xi) + \delta c_1(T, t, x, \xi) + \delta^2 c_2(T, t, x, \xi) + \dots, \\ u(T, t, x, \xi) &= u_0(T, t, x, \xi) + \delta u_1(T, t, x, \xi) + \dots, \\ \tilde{w}(T, t, x, \xi) &= \tilde{w}_0(T, t, x, \xi) + \delta \tilde{w}_1(T, t, x, \xi) + \dots, \\ p(T, t, x, \xi) &= p_0(T, t, x, \xi) + \delta p_1(T, t, x, \xi) + \dots, \end{aligned}$$

that remain uniformly valid over the slow timescale. We substitute into (4.1)–(4.4) and collect terms of each order.

4.1.1. $O(1)$ problem

At leading order we have

$$0 = -\frac{\partial p_0}{\partial x}, \tag{4.10}$$

$$0 = -\frac{\partial p_0}{\partial \xi} + \frac{\partial}{\partial x} \left(\eta_0 \frac{\partial \tilde{w}_0}{\partial x} \right), \quad \frac{\partial \tilde{w}_0}{\partial x} = 0 \text{ at } x = 0, \quad \tilde{w}_0 = -1 \text{ at } x = 1, \tag{4.11}$$

$$0 = \frac{\partial u_0}{\partial x} + \frac{\partial \tilde{w}_0}{\partial \xi}, \quad u_0 = 0 \text{ at } x = 0, 1, \tag{4.12}$$

$$0 = \frac{\partial^2 c_0}{\partial x^2}, \quad \frac{\partial c_0}{\partial x} = 0 \text{ at } x = 0, 1. \tag{4.13}$$

From (4.13) we see that c_0 has no x -dependence. We recall that

$$\dot{\gamma} = \left| \frac{\partial \tilde{w}}{\partial x} \right| + O([\delta/Pe]^2) \sim \left| \frac{\partial \tilde{w}_0}{\partial x} \right| + \delta \operatorname{sgn} \left(\frac{\partial \tilde{w}_0}{\partial x} \right) \frac{\partial \tilde{w}_1}{\partial x} + O(\delta^2) + O([\delta/Pe]^2).$$

Consequently, the leading-order viscosity is $\eta_0 = \eta(|\partial \tilde{w}_0/\partial x|; c_0, \eta_1, \eta_2, m)$. We see that p_0 is independent of x and hence integrating (4.13) we have

$$x \frac{\partial p_0}{\partial \xi} = \eta \left(\left| \frac{\partial \tilde{w}_0}{\partial x} \right|; c_0, \eta_1, \eta_2, m \right) \frac{\partial \tilde{w}_0}{\partial x}.$$

The right-hand side is the shear stress. For all the rheological models considered, the shear stress is a strictly monotone increasing function of $\dot{\gamma} > 0$. The viscosity function simply interpolates, with respect to c , between the effective viscosity of two such constitutive laws. Therefore, for fixed c_0 , the mixture shear stress will also be monotone with respect to $\dot{\gamma} = |\partial \tilde{w}_0/\partial x| > 0$. Thus, at fixed ξ the above relation can be inverted for any value of $\partial p_0/\partial \xi$, to give $\partial \tilde{w}_0/\partial x$ at each x . The pressure gradient, $\partial p_0/\partial \xi$, is determined from the requirement that

$$\int_0^1 \tilde{w}_0 \, dx = 0. \tag{4.14}$$

It can be shown that the flow rate integral above is a monotone function of $\partial p_0/\partial \xi$ and hence that a suitable $\partial p_0/\partial \xi$ can be found. Thus, \tilde{w}_0 can be computed. The transverse component of velocity, u_0 , can be obtained from (4.12). Finally, we observe that the dependence on (T, t, ξ) in the above procedure is only via $c_0(T, t, \xi)$, i.e. once $c_0(T, t, \xi)$ is known the entire leading-order solution can be obtained.

4.1.2. $O(\delta)$ problem

Hereafter we shall be primarily interested in determining higher-order corrections to the concentration, for which we will not need higher-order velocity perturbations.

The first-order concentration c_1 satisfies

$$\frac{\partial c_0}{\partial t} + \tilde{w}_0 \frac{\partial c_0}{\partial \xi} = \frac{\partial^2 c_1}{\partial x^2}, \quad \frac{\partial c_1}{\partial x} = 0 \text{ at } x = 0, 1. \tag{4.15}$$

We integrate (4.15) with respect to x over $[0, 1]$. The right-hand side vanishes due to the boundary conditions. On the left-hand side, c_0 is independent of x and by virtue of (4.14) the second term vanishes. Therefore, we have $\partial c_0/\partial t = 0$, and consequently

$$c_0 = c_0(T, \xi).$$

It also follows from §4.1.1 that the rest of the leading-order solution, (u_0, \tilde{w}_0, p_0) , is independent of t . Returning to (4.15), we now find

$$c_1(T, t, x, \xi) = c_1(T, t, 0, \xi) + \frac{\partial c_0}{\partial \xi}(T, \xi)h(T, x, \xi), \tag{4.16}$$

where

$$h(T, x, \xi) = \int_0^x \int_0^s \tilde{w}_0(T, y, \xi) \, dy \, ds. \tag{4.17}$$

4.1.3. $O(\delta^2)$ problem

At $O(\delta^2)$, we find that c_2 satisfies

$$\left. \begin{aligned} \frac{\partial c_0}{\partial T} + \frac{\partial c_1}{\partial t} + u_0 \frac{\partial c_1}{\partial x} + \tilde{w}_0 \frac{\partial c_1}{\partial \xi} &= \frac{\partial^2 c_2}{\partial x^2} + \frac{1}{Pe^2} \frac{\partial^2 c_0}{\partial \xi^2}, \\ \frac{\partial c_2}{\partial x} &= 0 \text{ at } x = 0, 1. \end{aligned} \right\} \tag{4.18}$$

Using (4.12) we replace $(u_0 \partial c_1/\partial x + \tilde{w}_0 \partial c_1/\partial \xi)$ by its conservative form $((\partial/\partial x)[u_0 c_1] + (\partial/\partial \xi)[\tilde{w}_0 c_1])$, and integrate (4.18) with respect to x over $[0, 1]$:

$$\frac{\partial c_0}{\partial T} + \frac{\partial c_1}{\partial t} + \int_0^1 \frac{\partial}{\partial \xi} [\tilde{w}_0 c_1] \, dx = \frac{1}{Pe^2} \frac{\partial^2 c_0}{\partial \xi^2}.$$

Note that although we have not computed \tilde{w}_1 , it must satisfy the zero-flux condition,

$$\int_0^1 \tilde{w}_1 \, dx = 0. \tag{4.19}$$

Now using (4.14), we write

$$\int_0^1 \frac{\partial}{\partial \xi} [\tilde{w}_0 c_1] \, dx = \frac{\partial}{\partial \xi} \left[\int_0^1 \tilde{w}_0 c_1 \, dx \right] = \frac{\partial}{\partial \xi} \left[\frac{\partial c_0}{\partial \xi}(T, \xi) \int_0^1 \tilde{w}_0(T, x, \xi)h(T, x, \xi) \, dx \right].$$

Thus, we have that

$$\frac{\partial c_0}{\partial T} + \frac{\partial c_1}{\partial t} = \frac{\partial}{\partial \xi} \left[\left(\frac{1}{Pe^2} + D_T(c_0) \right) \frac{\partial c_0}{\partial \xi} \right] \tag{4.20}$$

where D_T depends on c_0 via \tilde{w}_0 :

$$D_T(c_0) = - \int_0^1 \tilde{w}_0(T, x, \xi)h(T, x, \xi) \, dx. \tag{4.21}$$

In (4.20), $\partial c_1/\partial t = (\partial c_1/\partial t)(t, T, 0, \xi)$, is the only term that depends on t . Differentiating with respect to t we find that

$$\frac{\partial^2 c_1}{\partial t^2}(t, T, 0, \xi) = 0 \Rightarrow c_1(t, T, 0, \xi) = tA(T, \xi) + B(T, \xi).$$

However, we seek an asymptotic solution for which c_1 remains bounded for all t . Consequently, $A(T, \xi) = 0$ and we have

$$c_1 = c_1(T, x, \xi), \quad B(T, \xi) = c_1(T, 0, \xi).$$

The function $c_1(T, 0, \xi)$ will be determined from the secularity conditions at $O(\delta^3)$. The $O(\delta^3)$ problem is however algebraically complicated since it involves first-order velocity perturbations (which requires inclusion of the inertial terms and viscosity perturbations). It is also unnecessary to consider this problem in order to evaluate $(\partial c_1 / \partial x)(T, x, \xi)$, which is defined from (4.16), provided that $c_0(T, \xi)$ can be computed.

We now see that the secularity condition (4.20) simplifies to the following nonlinear diffusion equation for $c_0(T, \xi)$:

$$\frac{\partial c_0}{\partial T} = \frac{\partial}{\partial \xi} \left[\left(\frac{1}{Pe^2} + D_T(c_0) \right) \frac{\partial c_0}{\partial \xi} \right]. \tag{4.22}$$

Integration by parts yields

$$D_T = \int_0^1 \left(\int_0^x \tilde{w}_0(y, \xi) dy \right)^2 dx \geq 0, \tag{4.23}$$

from which we see that $D_T \geq 0$.

4.1.4. Summary of results

At leading order in the moving frame of reference, the concentration depends only on the slow time variable T and the axial coordinate ξ . Evolution of $c_0(T, \xi)$ is governed by the nonlinear diffusion equation (4.22). The diffusivity in (4.22) consists of two parts: the molecular diffusivity, which is represented by the term $1/Pe^2$, and a dispersive diffusivity D_T , which contains the effects of rapid diffusion across the channel (at leading order) followed by advection with the flow. Having computed $c_0(T, \xi)$ we can construct the leading-order solution, (u_0, \tilde{w}_0, p_0) , from §4.1.1. The first-order concentration gradient across the channel can also be found from $c_0(T, \xi)$ via (4.16).

4.2. Pipe flow displacements

An analogous analysis may be carried through for a displacement in a pipe. It is found that $c_0 = c_0(T, \xi)$, and again the nonlinear diffusion equation (4.22) is satisfied. However, now

$$h(T, r, \xi) = \int_0^r \left(\frac{1}{s} \int_0^s s_1 \tilde{w}_0(T, s_1, \xi) ds_1 \right) ds \tag{4.24}$$

and

$$D_T = - \int_0^1 2r \tilde{w}_0(T, r, \xi) h(T, r, \xi) dr = \int_0^1 \frac{2}{r} \left(\int_0^r s \tilde{w}_0(T, s, \xi) ds \right)^2 dr \geq 0. \tag{4.25}$$

The leading-order velocity and axial pressure gradient are found from

$$0 = - \frac{\partial p_0}{\partial r}, \tag{4.26}$$

$$0 = - \frac{\partial p_0}{\partial \xi} + \frac{1}{r} \frac{\partial}{\partial r} \left[r \eta_0 \frac{\partial \tilde{w}_0}{\partial r} \right], \quad \frac{\partial \tilde{w}_0}{\partial r} = 0 \text{ at } r = 0, \quad \tilde{w}_0 = -1 \text{ at } r = 1, \tag{4.27}$$

$$0 = \frac{1}{r} \frac{\partial}{\partial r} [r u_0] + \frac{\partial \tilde{w}_0}{\partial \xi}, \quad u_0 = 0 \text{ at } r = 0, 1, \tag{4.28}$$

with $\eta_0 = \eta(|\partial \tilde{w}_0 / \partial r|; c_0, \eta_1, \eta_2, m)$, and the axial pressure gradient chosen to satisfy the flow rate constraint

$$\int_0^1 r \tilde{w}_0 dr = 0. \quad (4.29)$$

The first-order concentration perturbation is given by

$$c_1(T, r, \xi) = c_1(T, 0, \xi) + h(T, r, \xi) \frac{\partial c_0}{\partial \xi}(T, \xi), \quad (4.30)$$

so that $c_{1,r}$ can again be evaluated from the leading-order concentration.

4.3. Comments on the asymptotic approximation for yield-stress fluids

In the case of yield-stress fluids, the leading-order shear-flow approximation, i.e. solving (4.11), will produce a leading-order velocity that has zero gradient over a central region of the flow. The naive interpretation that these regions represent unyielded plug regions is incorrect, as shown e.g. by Lipscomb & Denn (1984). These regions will instead be strained by the axial concentration gradient. This is manifested in extensional stresses within the pseudo-plug, which are of the same order of magnitude as the shear stresses. Although an $O(1)$ error is therefore incurred in predicting the deviatoric stress tensor, the error in the axial velocity within this region is $O(\varepsilon)$; see e.g. Balmforth & Craster (1999). For the purposes of dispersion, we can see that this is manifested in only an $O(\varepsilon)$ error in D_T , so that our method remains asymptotically consistent at leading order.

5. Taylor dispersion for generalized Newtonian fluids

In place of the diffusive displacement, let us suppose that fluid 1 and fluid 2 are identical. This corresponds to passive tracer advection, as considered by Taylor (1953) and Aris (1956). A rheological mixing law is redundant, \tilde{w}_0 is independent of the concentration and hence of (T, ξ) . Consequently the diffusivity D_T is constant. Long-time behaviour of the leading-order concentration c_0 , in the moving frame of reference, is governed by the linear diffusion equation:

$$\frac{\partial c_0}{\partial T} = \left[\frac{1}{Pe^2} + D_T \right] \frac{\partial^2 c_0}{\partial \xi^2}. \quad (5.1)$$

In dimensional terms, the leading-order concentration diffuses axially relative to the mean flow with an apparent axial diffusivity \hat{D}_a given by

$$\hat{D}_a = \hat{D} + D_T \frac{\hat{R}^2 \hat{U}_0^2}{\hat{D}}. \quad (5.2)$$

For a Newtonian fluid, we find that $D_T = 2/105$ for plane channel flow and $D_T = 1/48$ for pipe flow, which are the well-known classical results. The formulae (4.23) and (4.25) are also known as the general forms of Taylor dispersivity, for a given velocity. It is therefore reassuring that they are derived at leading order in our model of miscible displacement.

Computing D_T for any of the fluid models in §2.1 (or any other model) gives the corrected Taylor dispersion coefficient for a generalized Newtonian fluid. Computation of the axial velocity is relatively straightforward for each of these models, involving only simple quadrature and then solution of a single nonlinear equation for the axial pressure gradient; D_T then follows directly. For some of the rheological models, an

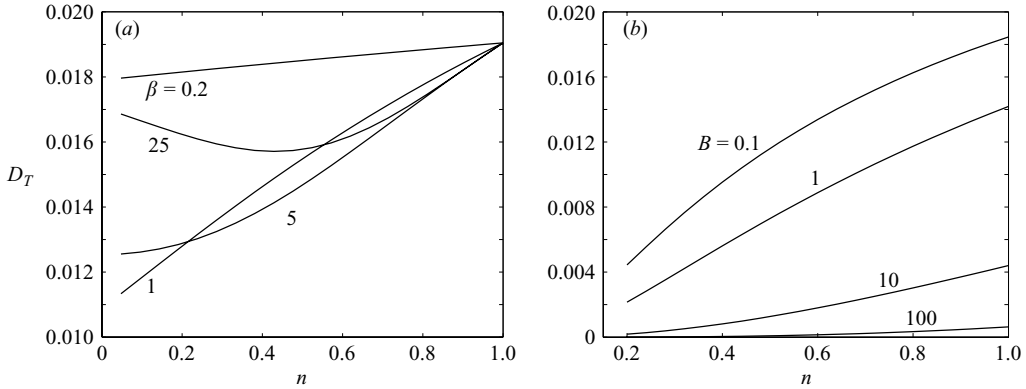


FIGURE 5. Plane-channel-flow Taylor dispersion coefficients: (a) Carreau fluid, $\alpha = 10$; (b) Herschel–Bulkley fluid.

analytical expression for D_T can be found, e.g. for the power-law fluid in a plane channel:

$$D_T = \frac{2}{3(2/n + 5)(1/n + 4)}. \tag{5.3}$$

In a pipe this becomes

$$D_T = \frac{1}{2(1/n + 5)(1/n + 3)}. \tag{5.4}$$

These results can be compared with Vartuli, Hulin & Daccord (1995).

We present also a selection of results that require numerical calculation. To generate the results presented, we compute pointwise values of \tilde{w}' to an accuracy 10^{-8} , integrate using Simpson’s rule with $\Delta x = 1/80$ to give the flow rate for given pressure drop, and then solve for the axial pressure drop to a tolerance 10^{-8} . Using this pressure drop we again integrate using Simpson’s rule to give \tilde{w} and again for D_T . Thus, the overall error is approximately 10^{-8} . The accuracy of the computation is verified analytically with the results for Newtonian and power-law fluids.

In figure 5 we present computed values of D_T for the plane channel, for the various models. Analogous results for the same fluid parameters, in a pipe flow, are shown in figure 6. Comparing figure 5 with figure 6, we see that pipe dispersion is qualitatively the same as that in the plane channel, for each rheological model; D_T is marginally larger for the pipe flow.

For passive scalar dispersion, D_T is a function solely of the axial velocity profile, $w = \tilde{w} + 1$. We can see directly from (4.23) and (4.25) that the dispersivity is reduced if the velocity profile is close to that of the mean flow. For example, as the power-law index n becomes small (shear-thinning), the power-law fluid axial velocity profile becomes progressively plug-like, and dispersion reduces. For the more complex models, the effects of shear-thinning are not always easy to pinpoint. For example, with the Carreau model the parameter $1/\beta$ relates to the range of rate of strain over which the model changes from low-shear to high-shear viscosity. However, for a particular imposed flow rate, the range of $\dot{\gamma}$ found will vary anyway. Since at both high and low shear the Carreau fluid has a Newtonian plateau in the effective viscosity, it is difficult to predict whether or not varying β will give more or less dispersion. As an example, figure 7(a) shows velocity profiles at $n = 0.1$ for various β .

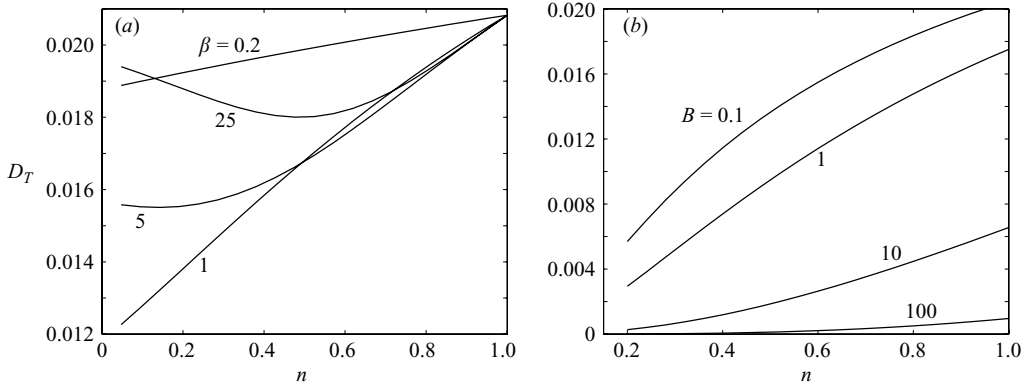


FIGURE 6. Pipe-flow Taylor dispersion coefficients: (a) Carreau fluid, $\alpha = 10$; (b) Herschel–Bulkley fluid.

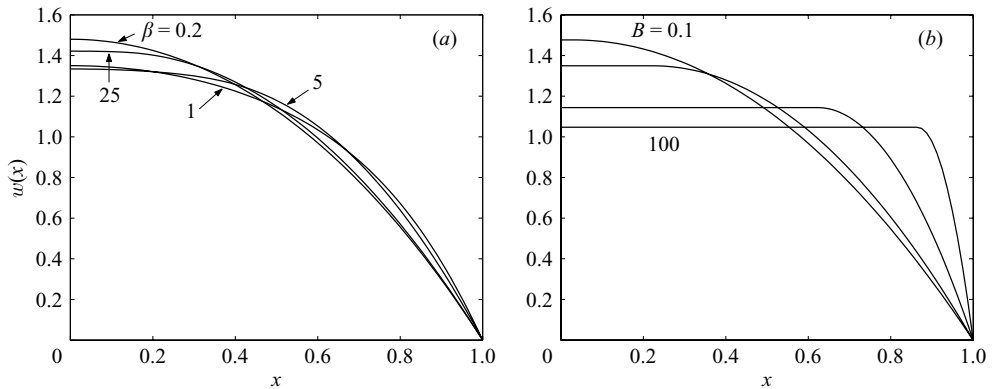


FIGURE 7. Axial velocity profiles: (a) Carreau fluid, $n = 0.1$, $\alpha = 10$, $\beta = 0.2, 1, 5, 25$; (b) Bingham fluid, $B = 0.1, 1, 10, 100$.

Both small and large β can increase dispersion and this ambiguity is reflected in the velocity profiles.

Apart from shear-thinning behaviour, the other phenomenon commonly observed with generalized Newtonian models concerns visco-plasticity: the fluid may be unyielded where the shear stress is below the yield stress. In terms of effects on dispersion, the velocity gradient is zero in unyielded regions, which reduces dispersion. Taking $n = 1$ in the Herschel–Bulkley model, we recover the popular Bingham model. Velocity profiles for successive B are shown in figure 7(b). The velocity is constant for $|x| < x^*$, where x^* is the position of the yield surface, which depends only on the Bingham number B . As $B \rightarrow \infty$ the velocity becomes progressively plug-like, $x^*(B) \rightarrow 1$, and dispersion is reduced. The following expression for the asymptotic behaviour is easily derived:

$$x^*(B) \sim 1 - \frac{\sqrt{2}}{B^{1/2}} + \frac{2}{3B} + O(B^{-3/2}), \tag{5.5}$$

from which we may deduce that $D_T(B) \sim 2/(3B)$ as $B \rightarrow \infty$. Similar asymptotic expressions can also be found for $n \neq 1$.

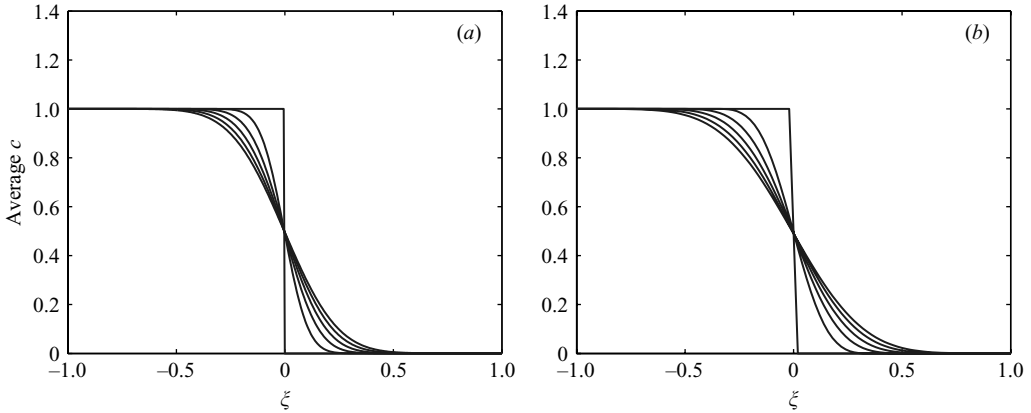


FIGURE 8. Average concentration of two Newtonian fluids, $m = 0.01$. (a) one-dimensional asymptotic model; (b) $\varepsilon Pe = 0.05$.

6. Displacements and nonlinear dispersion

We now turn to displacement of one fluid by another, i.e. c does not represent a passive tracer. This situation is modelled at leading order by the nonlinear diffusion equation (4.22). We comment that nonlinear diffusive effects may also enter through the molecular diffusivity, which often varies significantly with concentration, see e.g. Petitjeans & Maxworthy (1996) for the molecular diffusivity of a glycerine and water mixture. The analysis presented remains valid with $D(c)$:

$$D(c) = \frac{1}{Pe^2} D_m(c) + D_T(c),$$

for some order-unity positive function $D_m(c)$. Here however we shall assume $Pe \gg 1$, so that we may concentrate purely on the effects of the dispersion and mixing, i.e. the results we present formally consider $Pe \rightarrow \infty$.

Whereas Taylor dispersion is a well-established phenomenon and the linear diffusion results of §5 need no justification, here our first task is to verify that (4.22) does in fact predict long-time dispersive behaviour in the moving frame of reference. To this end, we shift the TFE model into the moving frame of reference and solve numerically (as outlined before) from initial conditions

$$c(x, \xi, 0) = 0 \text{ if } \xi > 0, \quad c(x, \xi, 0) = 1 \text{ if } \xi \leq 0.$$

For the fluid pairs considered earlier, we integrate until $t = (\varepsilon Pe)^{-1}$, for successively small εPe . The results $c(x, \xi, t)$ are averaged with respect to x and compared to the solution $c_0(T, \xi)$ of (4.22) at successive times. For both two-dimensional and one-dimensional computations, we have used the quarter-power mixing law for the results we present. The numerical method used to solve (4.22) is a predictor–corrector method due to Meek & Norbury (1982), that is second-order accurate in space and (nearly) second-order accurate in time. We have integrated using a spatial resolution $\Delta \xi = 0.005$ and fixed timestep $\Delta t = 0.0025$. The diffusivity $D_T(c)$ is evaluated at 100 regularly spaced values of c , with linear interpolation used between these values.

The results are shown in figures 8–10. In each case we can see that the one-dimensional asymptotic results closely resemble the two-dimensional results, integrated over the same time interval. Mean concentrations are plotted at $T = (\varepsilon Pe)t = 0, 0.2, 0.4, \dots, 1$. Note that there is no axial diffusion in the TFE

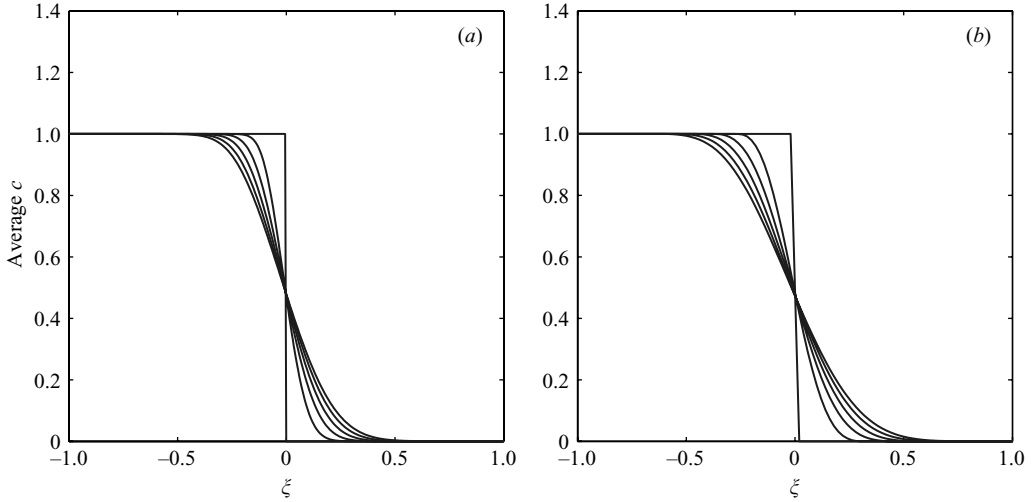


FIGURE 9. Average concentration of two power-law fluids, $n_1 = 0.8$, $n_2 = 0.4$, $m = 0.01$. (a) one-dimensional asymptotic model; (b) $\varepsilon Pe = 0.05$.

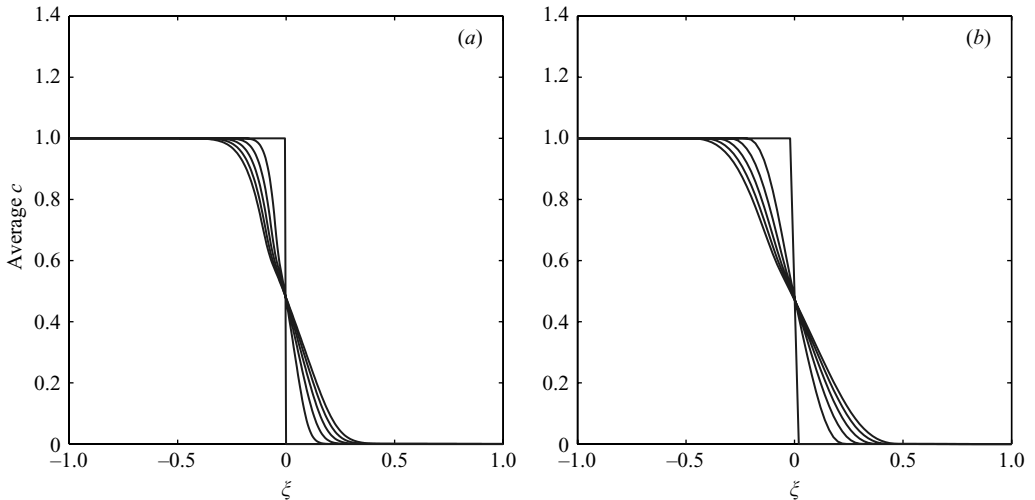


FIGURE 10. Average concentration of two Herschel–Bulkley fluids, $n_1 = 1$, $n_2 = 0.5$, $B_1 = 5$, $B_2 = 1$, $m = 0.01$. (a) one-dimensional asymptotic model; (b) $\varepsilon Pe = 0.05$.

model and we have eliminated this in the asymptotic model also by artificially taking $Pe \rightarrow \infty$. Therefore, the comparison is between dispersive effects in two dimensions and nonlinear diffusion in one dimension. Although close, the profiles are not identical. We attribute the small discrepancy to numerical diffusion effects for the two-dimensional computation. The two-dimensional computations become progressively time consuming as $\varepsilon Pe \rightarrow 0$, and it is unclear if numerical diffusion remains bounded in this limit. Hence our restriction to moderately small εPe in figures 8–10. Avoidance of such issues is one of the attractive features of the asymptotic approach.

The results in figures 8–10 strongly suggest that the multiple-scales technique is effective as an asymptotic approximation for this problem. We turn now to an exploration of the effects of non-passive mixing.

6.1. Effects of the mixing law

On ignoring molecular diffusion (or even in the common case when $Pe^2 \gg 1$), axial spreading of the mixture is governed by dispersive diffusion, manifested in $D_T(c)$. There are only a few general statements that can be made about $D_T(c)$, for any two given fluids. We may safely assert that: (i) $D_T(c) \geq 0$; (ii) $D_T(c)$ is continuous (smooth) with respect to c , provided that the mixing law is continuous (smooth); (iii) the end values of $D_T(c)$ at $c=0, 1$ are the Taylor dispersion values for the pure fluids.

The diffusivity $D_T(c)$ depends only on the rheological properties of the two fluids and on the mixing law that defines $\eta(\dot{\gamma}; c, \eta_1, \eta_2, m)$. Strictly speaking, these relations should be determined from experimental measurements. However broadly speaking, we may consider that pairs of fluids are either compatible or incompatible. By compatible fluids we mean that the constitutive laws are smoothly interpolated between those of the base fluids. The interpolation may of course be nonlinear, and (2.8) and (2.9) are reasonable models for this type of variation. A Newtonian example of this type of physical system would be a glycerine–water mixture.

Incompatible systems are also not hard to find. As one example, we may consider the concentration of NaOH in an aqueous Carbopol solution. Carbopol is mildly acidic and at low pH exhibits power-law behaviour. As the NaOH concentration is increased the solution is neutralized and shows yield stress for intermediate pH, i.e. effectively a Herschel–Bulkley fluid. Further increasing the NaOH concentration destroys the gel, and at high concentrations the solution is again approximately power law. We consider further such non-monotone effects in § 6.3.

For compatible systems, we would like to demonstrate that $D_T(c)$ can depend very sensitively on the mixing law. To illustrate this sensitivity, we have taken three different example fluid pairs and computed $D_T(c)$ using both (2.8) and (2.9). To illustrate the effects of the different $D_T(c)$, we then solve the nonlinear diffusion equation (4.22), for the two cases, starting at

$$c_0(\xi, 0) = 1, \quad \xi \leq 0; \quad c_0(\xi, 0) = 0, \quad \xi > 0.$$

The results are shown in figure 11, which depicts both $D_T(c)$ and the solution of (4.22), $c_0(\xi, T)$, at $T = 5$. For the first two fluid pairs in figure 11, there are only minor differences in the final concentrations. Note however that the total variation in $D_T(c)$ between the two fluids is not extreme, e.g. the Taylor dispersion coefficients are within a factor of 2 of each other. For the third fluid pair, there is a more extreme drop in diffusivity and consequently a significant difference in final concentration at $T = 5$.

6.2. Viscosity ratio, shear-thinning and yield-stress effects

The sensitivity of $D_T(c)$ to the mixing law may be viewed as both an inconvenience (in predicting behaviour) and an opportunity to control the extent of mixing. We should like therefore to understand how common non-Newtonian effects may affect $D_T(c)$, in as general terms as is possible. For generalized Newtonian fluids three effects that one might consider engineering (e.g. chemically) are to ‘viscosify’ the fluid, to affect the shear-thinning tendency of the mixture, or to introduce a yield stress. Below we examine these three effects individually. However, note that mathematically the problem is fairly well-defined. The condition for $D_T(c)$ to remain constant with a mixing law is that $w(x)$ be invariant. To produce large variations in $D_T(c)$ requires that the mixing law be suitably distant from the set of invariant mixing laws. This statement may not however be particularly helpful to a physical chemist. Equally, it is unrealistic to expect to be able to precisely engineer any desired optimal mixing law. Therefore, we consider more general effects.

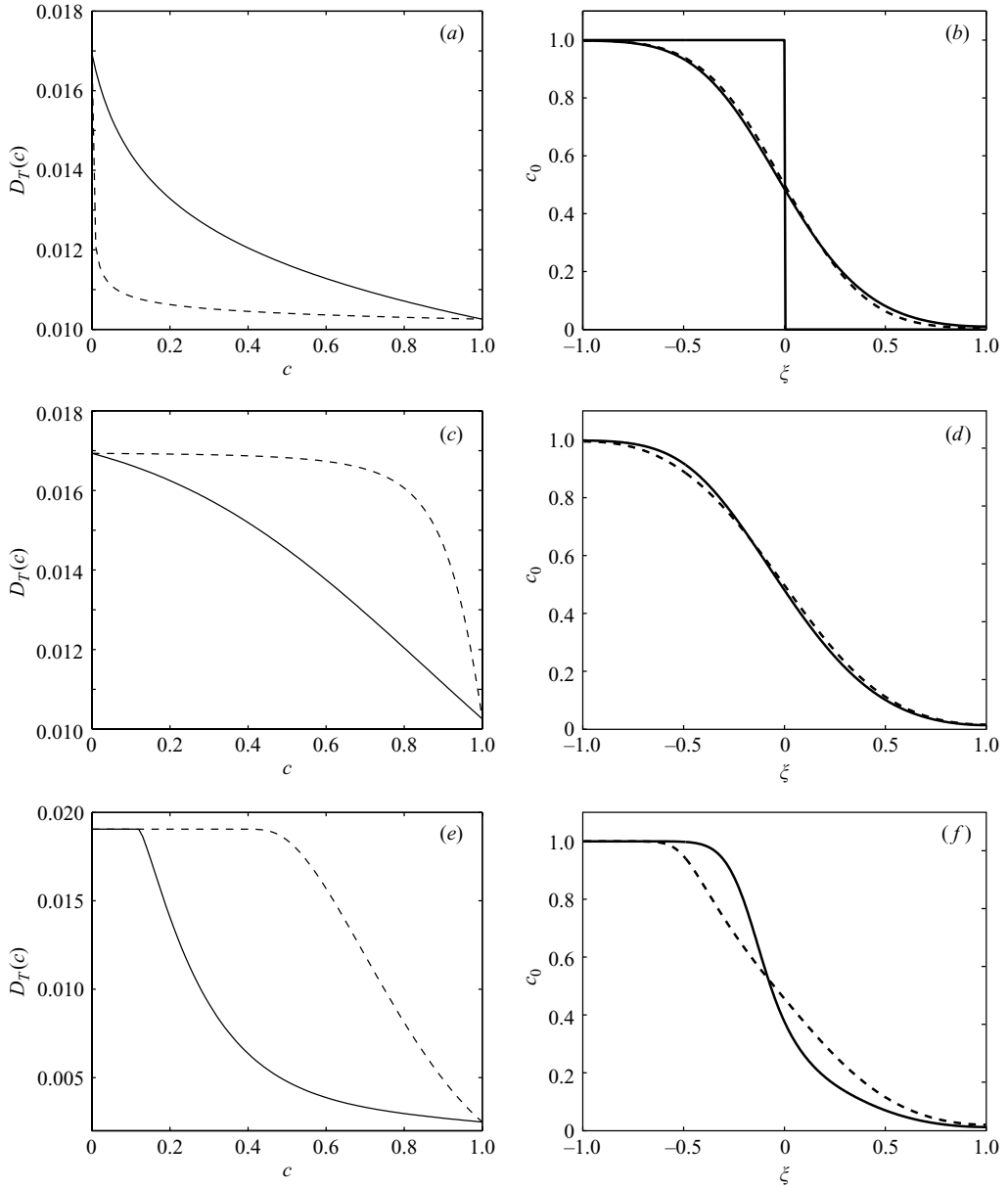


FIGURE 11. Effects of the mixing laws (2.9) and (2.8) on $D_T(c)$ and on the solution $c_0(\xi, T)$ of (4.22) at $T = 5$: (a, b) fluid 1, power law, $n = 0.8$, fluid 2, power law, $n = 0.4$, $m = 10$; (c, d) fluid 1, power law, $n = 0.8$, fluid 2, power law, $n = 0.4$, $m = 0.1$; (e, f) fluid 1, Newtonian, fluid 2, Herschel–Bulkley, $n = 0.5$, $B = 5$, $m = 1$. Dashed line (2.9), solid line (2.8).

By viscosification, we mean that we consider the effects of a change only in viscosity ratio m between two fluids of otherwise identical rheologies. Viscosification has little effect on the dispersion coefficient $D_T(c)$ for Newtonian fluids. This is because, with the mixing laws that we have assumed, the intermediate concentrations are also Newtonian fluids, which lead to an identical velocity profile. For other generalized Newtonian fluids, the effects of viscosification depend critically on the mixing law and the constitutive equations of the fluids: certain combinations will give $O(1)$ variations

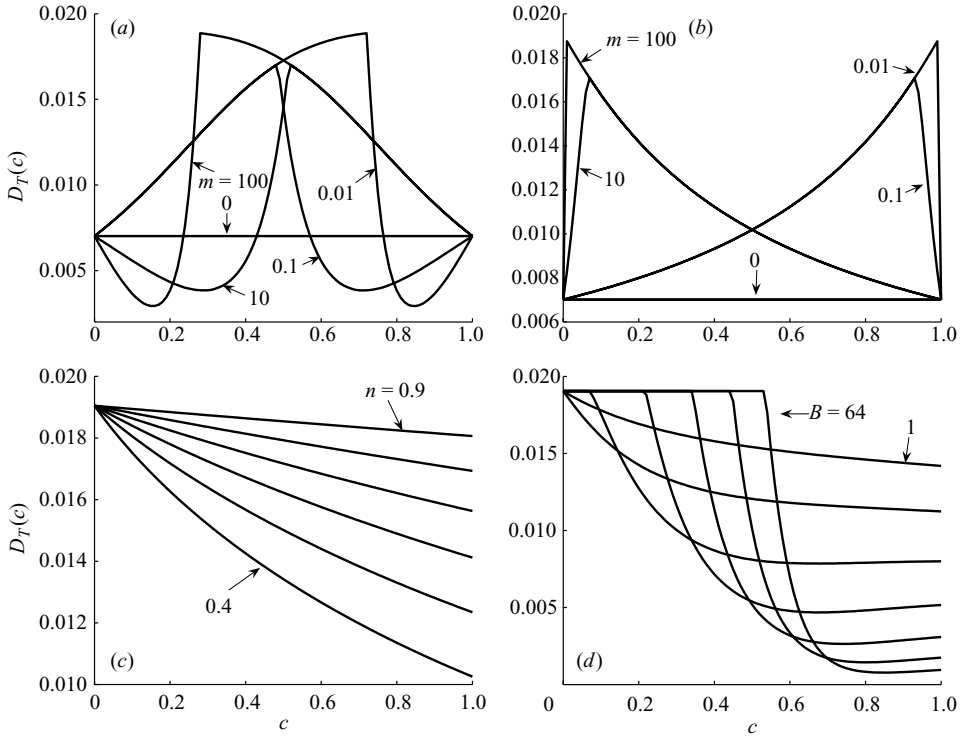


FIGURE 12. Taylor diffusivity $D_T(c)$. (a) Fluids 1 and 2, Bingham fluids, $B = 5$, mixing law (2.8), $m = 0.01, 0.1, 1, 10, 100$. (b) Fluids 1 and 2, Bingham fluids, $B = 5$, mixing law (2.9), $m = 0.01, 0.1, 1, 10, 100$. (c) Shear-thinning effects at $m = 1$: fluid 1 Newtonian, fluid 2 power law, index $n = 0.4, 0.5, \dots, 0.9$. (d) Yield stress effects at $m = 1$: fluid 1 Newtonian, fluid 2 Bingham, $B = 1, 2, 4, 8, 16, 32, 64$.

in dispersion, whereas others will not vary at all with m . Invariance of $D_T(c)$ is not equivalent to invariance of $\dot{\gamma}(\tau; c, \eta_1, \eta_2, m)$, since in general when we change the viscosity ratio, the pressure gradient (and hence shear stress) also changes, to satisfy the flow rate constraint. Examples of invariance are not hard to find. For example, for either (2.8) or (2.9), power-law fluids remain invariant to changes in m . To see this, observe that if $\eta_k = \dot{\gamma}_k^{n-1}$, then $\dot{\gamma} \propto \tau^{1/n} \propto x^{1/n}$ for either (2.8) or (2.9). The proportionality constant is determined from the unit flow rate constraint, hence is independent of m , and consequently so is the shape of the velocity profiles. Other fluid pairs do exhibit significant variations in $D_T(c)$ with m . We plot in figures 12(a) and 12(b), the effects of varying m for a Bingham fluid (Herschel–Bulkley model, $n = 1$), with $B = 5$. We show the different effects of the mixing laws, (2.8) and (2.9), in each figure. Although the effects on $D_T(c)$ are quite significant, they are not physically intuitive in any sense.

The effect of increased shear-thinning is to reduce dispersion, and this effect appears universal. One illustration is given in figure 12(c). In figure 12(d) we also show the effects of increasing the yield stress. Increasing the yield stress has a less obvious effect. At concentrations where the yield stress dominates in the mixture, $D_T(c)$ decreases with increasing yield stress. This effect is easily understood by reference to the velocity profiles in figure 7(b). For figure 12(c,d), we have used (2.8).

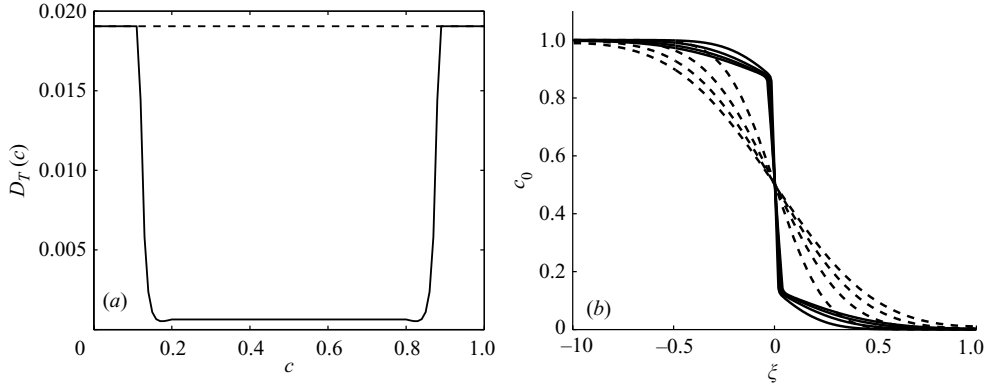


FIGURE 13. Model for a reactive fluid: (a) $D_T(c)$, fluids 1 and 2, Newtonian with $m=1$, (dashed line), with transition to Bingham fluid, $B=100$, for $0.2 \leq c \leq 0.8$ (solid line); (b) mean concentration profiles $c_0(\xi, T)$ at $T=1, 2, 3, 4$ for step initial condition, $D_T(c)$ as in (a).

6.3. Design of reactive fluids

Suppose now that we are able to design the rheology of the mixture. The results of the previous section give some clues as to the rheological behaviour that one should try to engineer in order to minimize dispersion. To experiment with this concept, we consider mixing between two Newtonian fluids that are ostensibly the same. Suppose that for a range of intermediate concentrations, the mixture develops a strong yield stress, e.g. this might be the case with a reactive system, an emulsion, or similar. For simplicity, we suppose that for $0.2 \leq c \leq 0.8$ the mixture behaves as a Bingham fluid, with $B=100$, and outside this range there is mixing according to (2.8) with Newtonian fluids.

Figure 13(a) shows the dispersive diffusivity $D_T(c)$, for the Newtonian–Newtonian mixture (dashed line), and the reactive modification discussed (solid line). At intermediate concentrations $D_T(c)$ drops drastically, as expected. In figure 13(b) we show the mean concentration profiles $c_0(\xi, T)$ at $T=1, 2, 3, 4$, obtained by solving the nonlinear diffusion equation (4.22), from a step-function initial condition. It is evident that the reactive mixture is very effective at limiting dispersion over the intermediate range of concentrations, and hence limiting spreading of the mixed zone. Similar effects can also be achieved by enhancing shear-thinning behaviour over a range of concentrations.

7. Conclusions

The chief contribution of this paper is in developing the asymptotic framework for the small- εPe limit of miscible duct displacements. The limit does not appear to have been explored previously. Our analysis has focused on providing a general framework that: (i) integrates seamlessly with the classical theories of dispersion for passive tracers; (ii) can be applied to a fairly broad class of non-Newtonian fluids common in industrial applications; (iii) can accommodate a broad range of mixing law closures for the rheology, either empirical or experimental.

The expression derived for the dispersive diffusivity (4.21) is easy to evaluate numerically for given generalized Newtonian rheologies and mixing law. Equally (4.20), although nonlinear, presents no difficulties numerically since $D(c)$ is strictly positive for finite Pe and B . We have shown numerically that the solutions of (4.20)

do approximate those of the two-dimensional TFE model in the limit of small εPe , validating the multiple-scales approach. Thus, (4.20) is a computationally economic model for investigating axial spreading.

In §5 we have shown the main effects of generalized Newtonian behaviour on Taylor dispersion, i.e. for a passive tracer. Qualitatively, these are mostly intuitive, i.e. D_T decreases with increasing yield stress or increased shear-thinning behaviour. As we have seen in §6, as soon as mixing occurs, the dispersive diffusivity begins to depend critically on the mixing law. This feature obviously causes practical difficulties if one's objective is to predict axial spreading. The root cause of this sensitivity is that certain mixing laws and rheological combinations lead to axial velocity profiles that are more or less sensitive to changes in the concentration. This sensitivity is transmitted directly from the velocity profile to $D_T(c)$.

Some of our results are not surprising, in that the classical dispersion results are found when a passive tracer is considered. However, the point of the paper is to make transparent the connection between miscible displacements and dispersion, so it would be disturbing if these results were not found. The perturbation approach offers a wider and consistent framework in which to model different physical effects that may influence miscible displacements. Here these effects have been those of a generalized Newtonian viscosity, but other rheological effects could be considered in the same framework.

J.Z. wishes to acknowledge financial support from the Pacific Institute for the Mathematical Sciences, via the award of PIMS postdoctoral fellowship, as well as funding from MITACS (Mathematics of Information Technology and Complex systems). I.F. acknowledges receipt of a research fellowship from the B.C. Advanced Systems Institute. Parts of this work have been completed under the overall direction of projects CRD-245434 (NSERC & Schlumberger Oilfield Services) and STPGP-306682 (NSERC, Schlumberger Oilfield Services & Trican Well Services). We are grateful for all financial support.

REFERENCES

- ALEXANDROU, A. N. & ENTOV, V. 1997 On the steady-state advancement of fingers and bubbles in a Hele-Shaw cell filled by a non-Newtonian fluid. *Eur. J. Appl. Math.* **8**, 73–87.
- ALLOUCHE, M., FRIGAARD, I. A. & SONA, G. 2000 Static wall layers in the displacement of two visco-plastic fluids in a plane channel. *J. Fluid Mech.* **424**, 243–277.
- ARIS, R. 1956 On the dispersion of a solute in a fluid flowing through a tube. *Proc. R. Soc. Lond. A* **235**, 67–78.
- AZAIEZ, J. & SINGH, B. 2002 Stability of miscible displacements of shear thinning fluids in a Hele-Shaw cell. *Phys. Fluids* **14**, 1557–1571.
- BAKHITIYAROV, S. & SIGINER, D. A. 1996 Fluid displacement in a horizontal tube. *J. Non-Newtonian Fluid Mech.* **65**, 1–15.
- BALMFORTH, N. J. & CRASTER, R. V. 1999 A consistent thin-layer theory for Bingham plastics. *J. Non-Newtonian Fluid Mech.* **84**, 65–81.
- BARENBLATT, G. I., ENTOV, V. M. & RYZHIK, V. M. 1990 Theory of fluid flows through natural rocks. In *Theory and Applications of Transport in Porous Media*, vol. 3, pp. 44–51, 187–229. Kluwer.
- BITTLESTON, S. H., FERGUSON, J. & FRIGAARD, I. A. 2002 Mud removal and cement placement during primary cementing of an oil well; laminar non-Newtonian displacements in an eccentric Hele-Shaw cell. *J. Engng Maths* **43**, 229–253.
- CHANG, S. H. & SLATTERY, J. C. 1986 A linear stability analysis for miscible displacements. *Transport in Porous Media* **1**, 179–199.

- CHEN, C.-Y. & MEIBURG, E. 1996 Miscible displacements in capillary tubes. Part 2. Numerical simulations. *J. Fluid Mech.* **326**, 57–90.
- CHEN, C.-Y. & MEIBURG, E. 2002 Miscible displacements in capillary tubes: Influence of Korteweg stresses and divergence effects. *Phys. Fluids* **14**, 2052–2058.
- COUSSOT, P. 1999 Saffman-Taylor instability in yield-stress fluids. *J. Fluid Mech.* **380**, 363–376.
- COX, G. 1962 On driving a viscous fluid out of a tube. *J. Fluid Mech.* **14**, 81–96.
- DACCORD, G., NITTMANN, J. & STANLEY, H. E. 1985 Radial viscous fingers and diffusion-limited aggregation: Fractal dimension and growth sites. *Phys. Rev. Lett.* **56**, 336–339.
- DIMAKOPOULOS, Y. & TSAMOPOULOS, J. 2003 Transient displacement of a viscoplastic material by air in straight and suddenly constricted tubes. *J. Non-Newtonian Fluid Mech.* **112**, 43–75.
- ERN, P., CHARRU, F. & LUCHINI, P. 2003 Stability analysis of a shear flow with strongly stratified viscosity. *J. Fluid Mech.* **496**, 295–312.
- FOWLER, A. C. 1998 *Mathematical Models in the Applied Sciences*, chap.13. Cambridge University Press.
- FRIGAARD, I. A., LEIMGRUBER, S. & SCHERZER, O. 2003 Variational methods and maximal residual wall layers. *J. Fluid Mech.* **483**, 37–65.
- FRIGAARD, I. A., SCHERZER, O. & SONA, G. 2001 Uniqueness and non-uniqueness in the steady displacement of two viscoplastic fluids. *Z. Angew. Math. Mech.* **81**, 9–118.
- GABARD, C. 2001 Etude de la stabilité de films liquides sur les parois d'une conduite verticale lors de l'écoulement de fluides miscibles non-newtoniens. These de l'Universite Pierre et Marie Curie (PhD thesis), Orsay, France.
- GABARD, C. & HULIN, J.-P. 2003 Miscible displacements of non-Newtonian fluids in a vertical tube. *Eur. Phys. J. E* **11**, 231–241.
- HICKERNELL, F. J. & YORTSOS, Y. C. 1986 Linear stability of miscible displacement processes in porous media in the absence of dispersion. *Stud. Appl. Maths* **74**, 93–115.
- JIANG, G.-S., LEVY, D., LIN, C.-T., OSHER, S. & TADMOR, E. 1988 High-resolution nonoscillatory central schemes with nonstaggered grids for hyperbolic conservation laws. *SIAM J. Numer. Anal.* **35**, 2147–2168.
- JIANG, G.-S. & TADMOR, E. 1998 Nonoscillatory central schemes for multidimensional hyperbolic conservation laws. *SIAM J. Sci. Comput.* **19**, 1892–1917.
- JOSEPH, D. D. & RENARDY, Y. Y. 1993 *Fundamentals of Two-Fluid Dynamics. Part II: Lubricated transport, drops and miscible liquids*. Interdisciplinary Applied Mathematics, vol. 4, pp. 324–360. Springer.
- KAWAGUCHI, M., MAKINO, K. & KATO, T. 1997 Viscous fingering patterns in polymer solutions. *Physica D* **109**, 325–332.
- KONDIC, L., PALFFY-MUHORAY, P. & SHELLEY, M. J. 1996 Models of non-Newtonian Hele-Shaw flow. *Phys. Rev. E* **54**, 4536–4539.
- KONDIC, L., SHELLEY, M. J. & PALFFY-MUHORAY, P. 1998 Non-Newtonian Hele-Shaw flow and the Saffman-Taylor instability. *Phys. Rev. Lett.* **80**, 1433–1436.
- LAJEUNESSE, E. 1999 Déplacement et instabilités de fluides miscibles et immiscibles en cellules de Hele-Shaw. These de l'Universite Pierre et Marie Curie (PhD thesis), Orsay, France.
- LAJEUNESSE, E., MARTIN, J., RAKOTOMALALA, N. & SALIN, D. 1997 3D Instability of miscible displacements in a Hele-Shaw cell. *Phys. Rev. Lett.* **79**, 5254–5257.
- LAJEUNESSE, E., MARTIN, J., RAKOTOMALALA, N. & SALIN, D. 2001 The threshold of the instability in miscible displacements in a Hele-Shaw cell at high rates. *Phys. Fluids* **13**, 799–801.
- LAJEUNESSE, E., MARTIN, J., RAKOTOMALALA, N., SALIN, D. & YORTSOS, Y. 1999 Miscible Displacement in a Hele Shaw Cell at High Rates. *J. Fluid Mech.* **398**, 299–319.
- LINDNER, A. 2000 L'instabilité de Saffman-Taylor dans les fluides complexes: relation entre les propriétés rhéologiques et la formations de motifs. These de l'Universite Paris VI (PhD thesis), Paris, France.
- LINDNER, A., COUSSOT, P. & BONN, D. 2000 Viscous fingering in a yield stress fluid. *Phys. Rev. Lett.* **85**, 314.
- LIPSCOMB, G. G. & DENN, M. M. 1984 Flow of Bingham fluids in complex geometries. *J. Non-Newtonian Fluid Mech.* **14**, 337–346.
- LIU, S. & MASLIYAH, J. H. 1999 Nonlinear flows in porous media. *J. Non-Newtonian Fluid Mech.* **86**, 229–252.

- MANICKAM, O. & HOMSY, G. M. 1993 Stability of miscible displacements in porous media with nonmonotonic viscosity profiles. *Phys. Fluids* **5**, 1356–1367.
- MEEK, P. C. & NORBURY, J. 1982 Two-stage, two-level finite difference schemes for non-linear parabolic equations. *IMA J. Numer. Anal.* **2**, 335–356.
- MUSKAT, M. 1937 *The Flow of Homogeneous Fluids through Porous Media*. McGraw-Hill.
- NITTMANN, J., DACCARD, G. & STANLEY, H. E. 1985 Fractal growth of viscous fingers: Quantitative characterization of a fluid instability phenomenon. *Nature* **314**, 141–144.
- PASCAL, H. 1984a Rheological behaviour effect of non-Newtonian fluids on dynamic of moving interface in porous media. *Intl J. Engng Sci.* **22**, 227–241.
- PASCAL, H. 1984b Dynamics of moving interface in porous media for power law fluids with a yield stress. *Intl J. Engng Sci.* **22**, 577–590.
- PASCAL, H. 1986 A theoretical analysis of stability of a moving interface in a porous medium for Bingham displacing fluids and its application in oil displacement mechanism. *Can. J. Chem. Engng* **64**, 375–379.
- PELIPENKO, S. & FRIGAARD, I. A. 2004a On steady state displacements in primary cementing of an oil well. *J. Engng Maths* **48**, 1–26.
- PELIPENKO, S. & FRIGAARD, I. A. 2004b Two-dimensional computational simulation of eccentric annular cementing displacements. *IMA J. Appl. Maths* **64**, 557–583.
- PELIPENKO, S. & FRIGAARD, I. A. 2004c Visco-plastic fluid displacements in near-vertical narrow eccentric annuli: prediction of travelling-wave solutions and interfacial instability. *J. Fluid Mech.* **520**, 343–377.
- PETITJEANS, P. & MAXWORTHY, T. 1996 Miscible displacements in capillary tubes. Part 1. Experiments. *J. Fluid Mech.* **326**, 37–56.
- RAKOTOMALALA, N., SALIN, D. & WATZKY, P. 1997 Miscible displacement between two parallel plates: BGK lattice gas simulations. *J. Fluid Mech.* **338**, 277–297.
- ROGERSON, A. & MEIBURG, E. 1993a Shear stabilization of miscible displacement processes in porous media. *Phys. Fluids A* **5**, 1344–1355.
- ROGERSON, A. & MEIBURG, E. 1993b Numerical simulation of miscible displacement processes in porous media flows under gravity. *Phys. Fluids A* **5**, 2644–2660.
- SADER, J. E., CHAN, D. Y. C. & HUGHES, B. D. 1994 Non-Newtonian effects on immiscible viscous fingering in a radial Hele-Shaw cell. *Phys. Rev. E* **49**(1), 420–432.
- SAFFMAN, P. G. & TAYLOR, G. I. 1958 The penetration of a finger into a porous medium in a Hele-Shaw cell containing a more viscous liquid. *Proc. R. Soc. Lond. A* **245**, 312.
- SCOFFONI, J., LAJEUNESSE, E. & HOMSY, G. M. 2001 Interfacial instabilities during displacements of two miscible fluids in a vertical pipe. *Phys. Fluids* **13**, 553–556.
- TAN, C. T. & HOMSY, G. M. 1986 Stability of miscible displacements in porous media: Rectilinear flow. *Phys. Fluids* **29**, 3549.
- TAN, C. T. & HOMSY, G. M. 1988 Simulation of nonlinear viscous fingering in miscible displacement. *Phys. Fluids* **31**, 1330–1336.
- TARDY, P. M. J. & PEARSON, J. R. A. 2002 Models for flow of non-Newtonian and complex fluids through porous media. *J. Non-Newtonian Fluid Mech.* **102**, 447–473.
- TAYLOR, G. I. 1953 Dispersion of soluble matter in a solvent flowing slowly through a tube. *Proc. R. Soc. Lond. A* **219**, 186–203.
- TAYLOR, G. I. 1961 Deposition of a viscous fluid on the wall of a tube. *J. Fluid Mech.* **10**, 161–165.
- VARTULI, M., HULIN, J.-P. & DACCARD, G. 1995 Taylor dispersion in a polymer solution flowing through in a capillary tube. *AIChE J.* **41**, 1622–1628.
- WILSON, S. D. R. 1990 The Taylor-Saffman problem for a non-Newtonian liquid. *J. Fluid Mech.* **220**, 413–426.
- YANG, Z. & YORTSOS, Y. C. 1997 Asymptotic solutions of miscible displacements in geometries of large aspect ratio. *Phys. Fluids* **9**, 286–298.
- YORTSOS, Y. C. 1987 Stability of displacement processes in porous media in radial flow geometries. *Phys. Fluids* **30**, 2928–2935.
- YORTSOS, Y. C. & ZEYBEK, M. 1988 Dispersion driven instability in miscible displacement in porous media. *Phys. Fluids* **31**, 3511–3518.
- ZIMMERMAN, W. B. & HOMSY, G. M. 1992 Viscous fingering in miscible displacements: Unification of effects of viscosity contrast, anisotropic dispersion, and velocity dependence of dispersion on nonlinear finger propagation. *Phys. Fluids A* **4**, 2348–2359.